PALEOENVIRONMENTAL ANALYSIS OF COASTAL MARSH DEPOSITS IN THE AGUJA FORMATION, LATE CRETACEOUS, TRANS-PECOS TEXAS

by

RICHARD STOREY RECORD, B.S.

A THESIS

IN

GEOLOGY

Submitted to the Graduate Faculty
of Texas Tech University in
Partial Fulfillment of
the Requirements for
the Degree of

MASTER OF SCIENCE

Approved

December, 1988

ACKNOWLEDGEMENTS

The path to this point has been somewhat less than straight. I thank my parents for sticking with the kid who never seemed to take advantage of his ability. I thank them also for giving me the time to figure out the path I wanted, and their support when I stepped off the side for awhile. The rest of my family deserves added thanks for being there. I always know I have their support, and their good-natured needling let me know that this was important to them also.

I am indebted to Dr. Thomas M. Lehman for taking me on when my first venture crashed. The help he has given has been invaluable. Susan Ensenat, Bill Slopey, Brian Moore, my "cuz," and many others in the department have all been a source of happiness. Darrell Brownlow deserves added thanks for analyzing my clays quickly and thoroughly. Dr. Gary E. Strathearn, Dr. Calvin Barnes, and Dr. James E. Barrick deserve credit for technical assistance and critical review. Big Bend National Park officials allowed access to outcrop exposures and sample collecting.

TABLE OF CONTENTS

ABSTRACT

Upper Cretaceous carbonaceous shale, lignite, and coal deposits of the Aguja Formation are exposed on the southwest flank of Rattlesnake Mountain in western Big Bend National Park. These deposits represent accumulation in delta plain marshes and swamps. Variations in depositional environment ranging from prograding delta plain marsh sediments to well-drained swamp deposits are distinguished among the lower, middle, and upper shale members of the Aguja.

Lithologic analysis, clay mineralogy, total organic carbon analysis, stable carbon and oxygen isotopic analysis, thin section petrography, and palynology are employed to differentiate facies. On the basis of this facies analysis prograding delta plain marsh environments are interpreted for the lower and middle shale members. The upper shale member is proposed to represent deposition in a well-drained swamp environment. Lithologic variations and a relationship between kaolinite and total organic carbon indicates cyclicity in the lower and middle shale members.

The lower shale member overlies the progradational basal sandstone member of the Aguja, and represents deposition in a delta plain marsh with crude cyclicity

apparent in the facies found. Lignitic layers cap the marsh cycles, and kaolinite enrichment is found below the lignites.

The middle shale member overlies the transgressive Rattlesnake Mountain sandstone member, and is similar in lithology to the lower shale member. The middle shale member consists of carbonaceous shale and lignite, and may represent marsh progradation over the Rattlesnake Mountain sandstone.

The upper shale member overlies the Terlingua Creek sandstone member, and represents a departure from marsh deposition. In situ stumps, logs, and sparse organic material in the shale indicate deposition in a well-drained swamp, perhaps in a proximal deltaic environment.

LIST OF TABLES

TABLES

LIST OF FIGURES

FIGURES

CHAPTER I

INTRODUCTION

The Upper Cretaceous Aguja Formation consists of an alternating series of shale and sandstone beds deposited in open and restricted shallow sublittoral environments, coastal swamps and marshes, estuaries, deltas, and fluvial floodplains (Lehman, 1985). These sediments accumulated along the western shore of the Cretaceous Interior Seaway during Campanian and Maastrichtian time. The Aguja Formation is well exposed in and around Big Bend National Park, in Brewster County, Texas. Aguja exposures on the southwest flank of Rattlesnake Mountain, in the west end of Big Bend, are the focus of the present study (Figure 1a).

The Aguja Formation overlies the Pen Formation. The contact is marked by the prominent basal sandstone member of the Aguja. The Aguja Formation is divided into six informal members (Figures 1b and 2). The lower shale member rests above the basal sandstone member and is overlain by the Rattlesnake Mountain sandstone member. The middle shale member overlies this sandstone and is itself overlain by the Terlingua Creek sandstone member. The Aguja section is capped by the upper shale member, which is overlain by the Javelina Formation. Laterally,

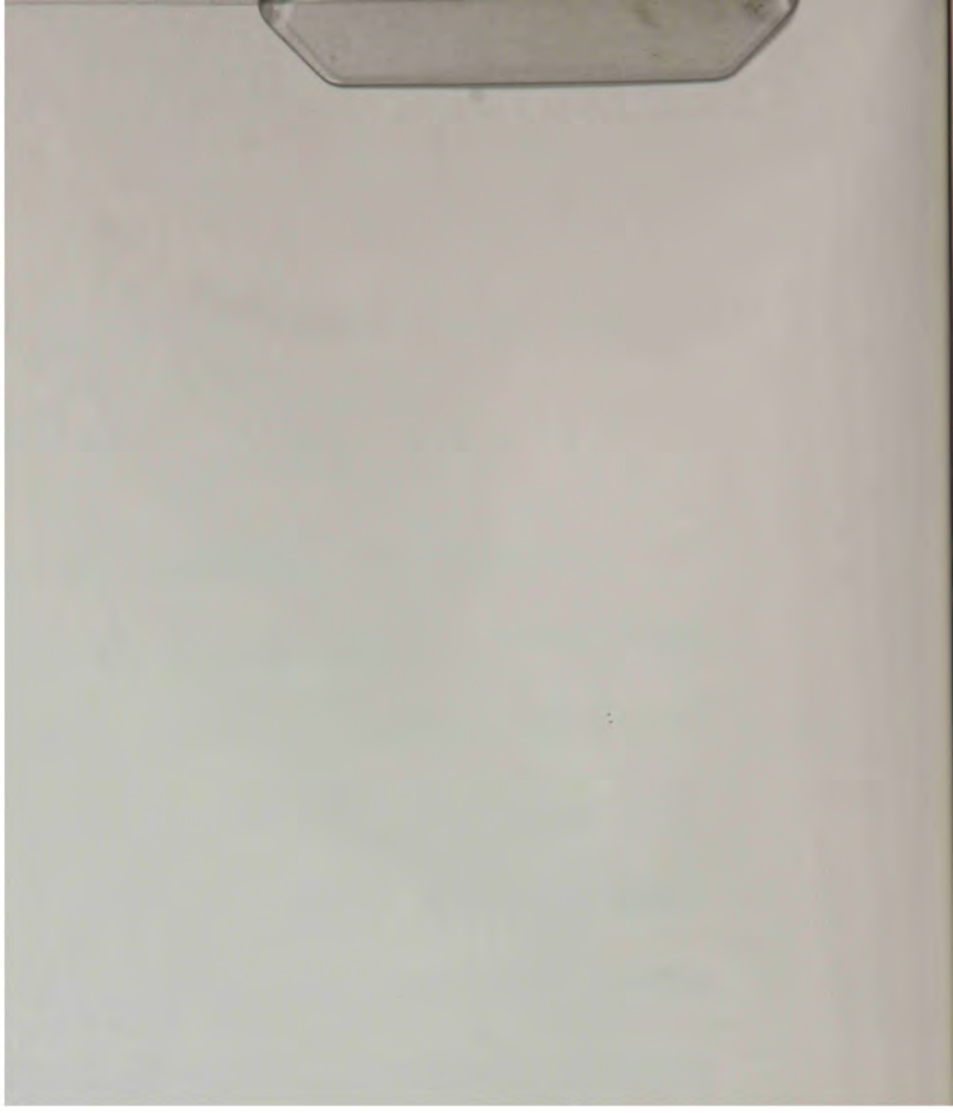

Figure 1. Location of study area within Big Bend National Park, and stratigraphic nomenclature for Upper Cretaceous sedimentary rocks in the Big Bend region (after Lehman, 1985).

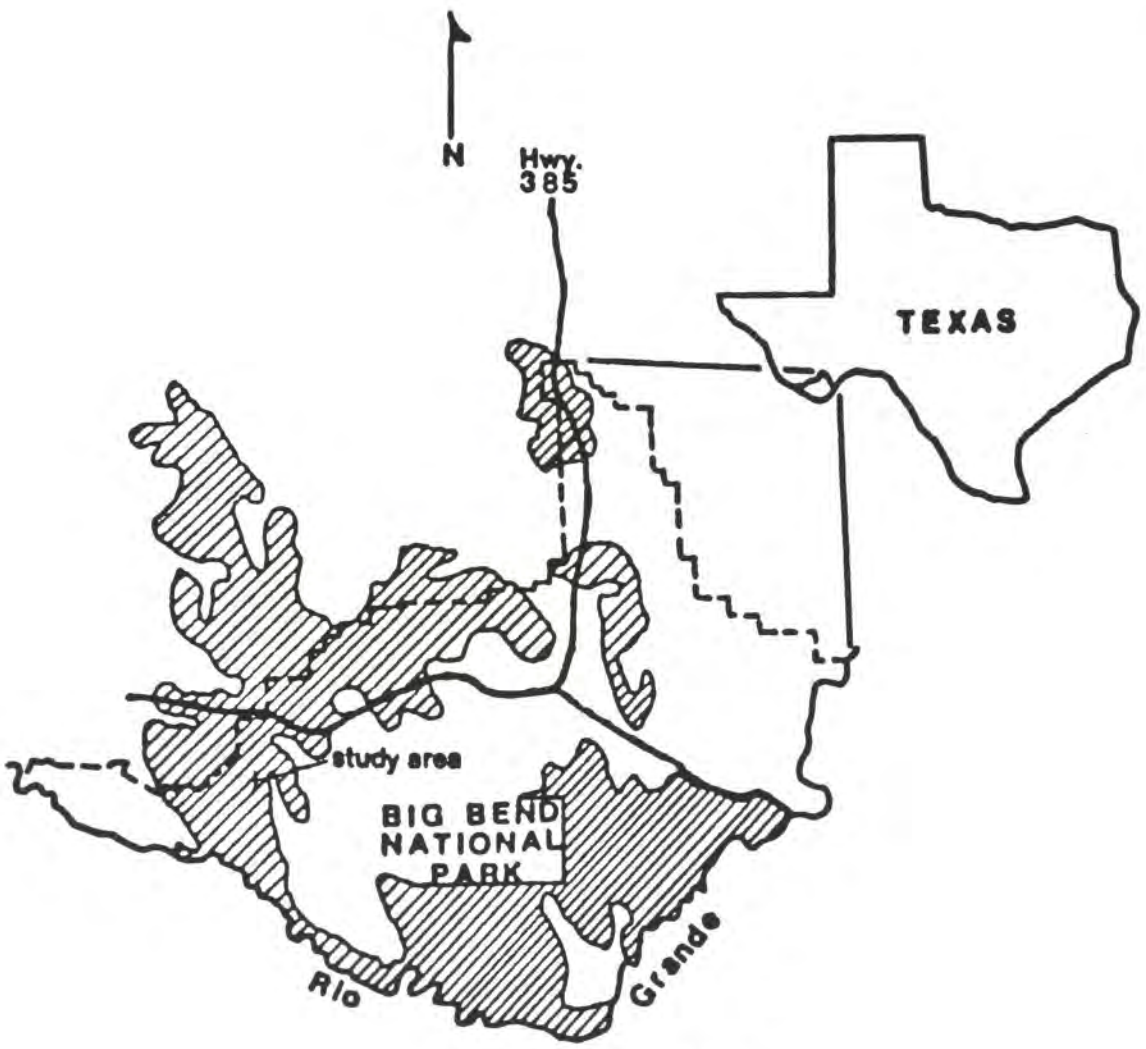
N
Hwy. 385
TEXAS
study area
BIG BEND NATIONAL PARK
Rio Grande
0
20 km

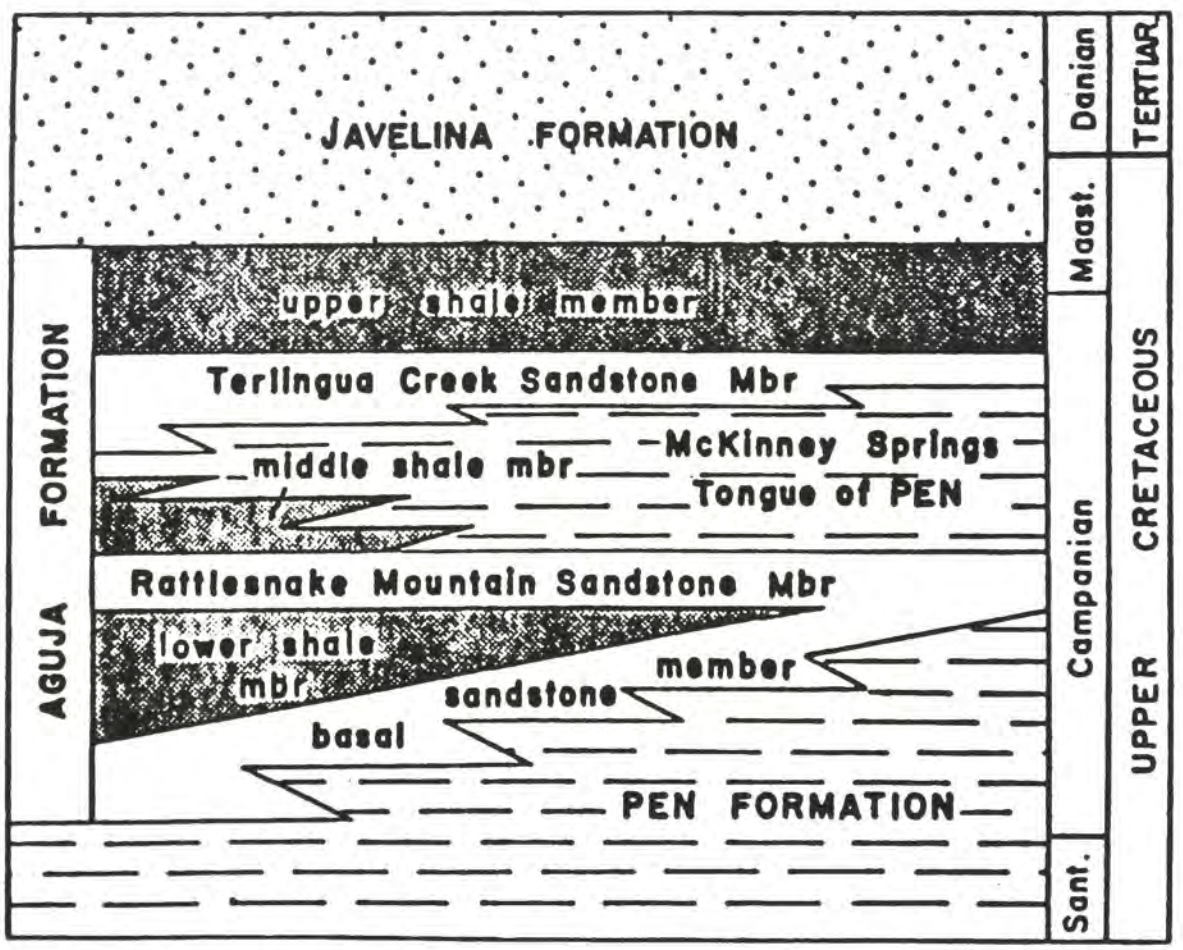
JAVELINA FORMATION
upper shale member
Terlingua Creek Sandstone Mbr
McKinney Springs
middle shale mbr
Tongue of PEN
Rattlesnake Mountain Sandstone Mbr
lower shale mbr
member
sandstone
basal
PEN FORMATION
AGUJA FORMATION
Danian
Maast.
Campanian
Sant.
TERTIAR
UPPER CRETACEOUS

Figure 2. The six informal members of the Aguja Formation, (from left to right) the basal sandstone member, lower shale member, Rattlesnake Mountain sandstone member, middle shale member, Terlingua Creek sandstone member, and upper shale member (man in lower left as scale).

these units intertongue with each other (Figure 1b), and record the shifting position of the shoreline of the Cretaceous Interior Seaway (Lehman, 1985).

The purpose of this study is to document in detail the environments of deposition of the lower and middle shale members of the Aguja Formation and determine what, if any, cyclicity exists in the section. Analysis of cycles in the section may aid in determination of environmental changes in the deposits. It should also be possible to determine if the lignite layers are random events or can be related to environmental changes. Hand sample analysis, clay mineralogy, total organic carbon analysis, stable carbon and oxygen isotopic analysis, thin section petrography, and palynology are employed to differentiate facies. A vertical section through the Aguja on Rattlesnake Mountain (Figure 3) is described and analyzed in detail to determine the depositional history of the sediments. The lower and middle shale members display a crude cyclicity reflected by alternating shale and lignite layers, and an apparent relationship between clay mineralogy and total organic carbon content.

Geologic Setting

Late Cretaceous sedimentation in the Trans-Pecos region of Texas was affected by regional tectonism and

Figure 4. General vertical section "S" through the six members of the Aguja Formation. A - C' represent cycles in the lower shale member, and symbols represent various features found in the section.

Figure 3. Geologic map of the study area on the southwest flank of Rattlesnake Mountain showing the location of section "S" (after Lehman, 1985).

GEOLOGIC MAP OF RATTLESNAKE MOUNTAIN VICINITY, BIG BEND NATIONAL PARK, BREWSTER COUNTY, TEXAS

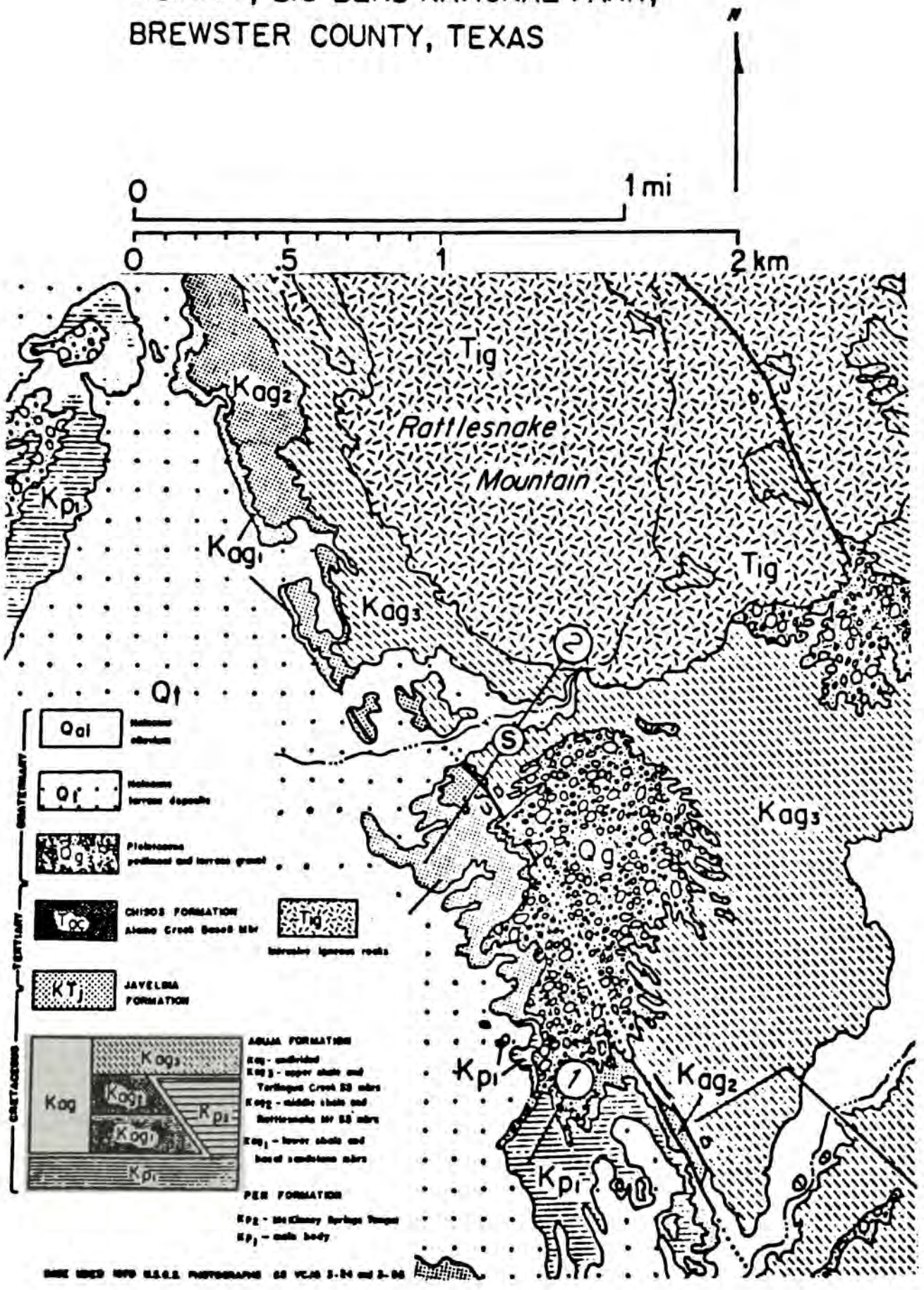

volcanism. A volcanic arc in western Mexico provided detrital sediments to the Trans-Pecos region (McDowell and Clabaugh, 1979). Transgressive-regressive cycles recognized in the Cretaceous Interior Seaway can be correlated with those observed in Trans-Pecos sedimentation. Northeastward progradation of the Late Cretaceous shoreline is indicated by thinning of the Pen Formation, and paleocurrent data from the lower parts of the Aguja Formation (Lehman, 1985). Thinning of the basal sandstone member to the northeast, and its absence at Persimmon Gap, Black Gap, and San Vicente indicates a terminus of initial Aguja progradation just east of the present location of the Santiago-Sierra del Carmen range (Lehman, 1985). The McKinney Springs tongue of the Pen Formation, which is laterally equivalent to the middle shale member of the Aguja Formation, reflects renewed marine transgression. Another episode of northeastward progradation deposited the Terlingua Creek sandstone member and upper shale member of the Aguja Formation. Javelina Formation deposition followed this progradation, and reflects sedimentation on a fluvial floodplain (Lehman, 1985).

Previous Work

Strata of the Aguja Formation were originally named the "Rattlesnake Beds" by Udden (1907) for Rattlesnake

Mountain in Big Bend. Adkins (1933) renamed these strata the Aguja Formation, and designated Sierra Aguja as the type locality. No type section was described by either worker, but a series of sections measured by Udden near Chisos Pen serve as the type section (Lehman, 1985). Maxwell et al. (1967) divided the Aguja into a lower marine unit, and an upper nonmarine unit. Kovschak (1973) utilized a similar scheme, but included a middle transitional facies. The Aguja was divided into a lower, middle, and upper member by Knebush (1981). Lehman (1982) similarly divided the formation into the basal sandstone, lower shale, medial sandstone, and upper shale divisions. Lehman (1985) redefined these divisions as six informal members consisting of the basal sandstone member, lower shale member, Rattlesnake Mountain sandstone member, middle shale member, Terlingua Creek sandstone member, and upper shale member. Bohanan (1987) studied the basal sandstone member and Terlingua Creek sandstone member of the Aguja near McKinney Springs in the Park. Schroeder (in progress) studied the Terlingua Creek sandstone near Grapevine Hills in the Park. Bohanan and Schroeder subdivide these units into deltaic sedimentary facies, and discuss variations in sandstone diagenesis that correlate with facies changes. The stratigraphic terminology developed by Lehman (1985) is followed in this report.

CHAPTER II

LITHOLOGY

A stratigraphic section through the Aguja Formation on Rattlesnake Mountain (Figure 4) is described in this chapter. The section begins at the basal sandstone member and ends 50 meters into the upper shale at the top of a prominent ledge-forming conglomeratic sandstone. The symbols to the right of the section indicate interesting material found in the section, and gives the approximate location where they were collected. For example, one symbol shows the locations where bones of a brackish-water crocodile (Deinosuchus) were found. In this study, the shale units are described in detail, with emphasis on the lower and middle shale members.

Methods

Sample Collection

Shale samples were collected throughout a vertical section of the outcrop at locations exhibiting color variation or where other lithologic changes occurred. The subtle color changes are masked in most places by the slumped yellow to gray weathered surface. It was therefore necessary to dig into the exposure at intervals

Figure 4. General vertical section "S" through the six members of the Aguja Formation. A - C' represent cycles in the lower shale member, and symbols represent various features found in the section.

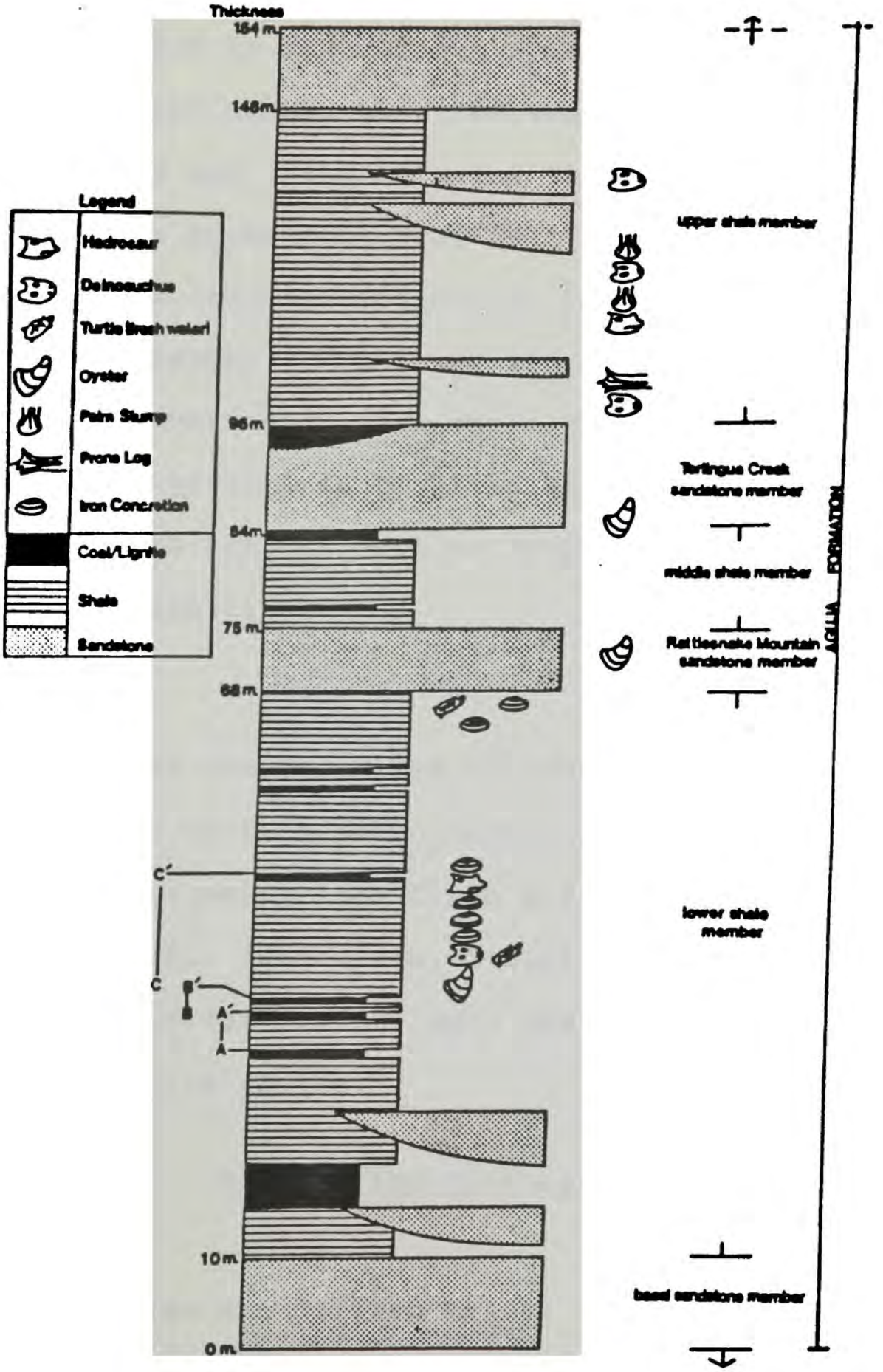
Thickness
154 m.
148m.
96 m.
84m.
75 m.
68 m.
10m.
0 m.
Legend
Hadrosaur
Deinosuchus
Turtle (fresh water)
Oyster
Palm Stump
Prone Log
Iron Concretion
Coal/Lignite
Shale
Sandstone
C'
C
A'
A
upper shale member
Tertiguas Creek sandstone member
middle shale member
Rattlesnake Mountain sandstone member
lower shale member
basal sandstone member
AGUJA FORMATION

of a meter or less to see the fresh unweathered surface (sample numbers in appendix).

Differences in the various shale lithologies are apparent in hand sample when the weathered surface is excavated away and fresh material is obtained. The shales range in color from light gray (N7) to brownish black (5 YR 2/1) with a few pale red purple (5 RP 6/2) units in the middle shale member. The lower and middle shales appear to be more carbonaceous as a whole than the upper shale, and in places grade into lignites and subbituminous coals. The shales also exhibit various degrees of lamination, luster, and fissility.

Analysis

The shales are described through hand sample analysis, thin section petrography, X-ray diffractometry, and mass spectrometry (see Clays and Total Organic Carbon chapter). Color, lamination, luster, and visible content of organic material are the main features used to distinguish shale facies.

Results and Discussion

Lithologies

Nine facies are defined below. In the following chapters each of the analytical techniques is described. The shales within each facies show variation in

lamination, luster, and kaolinite content, but are similar in color and total organic carbon content. There is significant overlap in kaolinite content between groups, but the samples in each group tend to cluster loosely together. Four of the lithologic units (VI-IX) meet the definition of coal. Coal is defined as, "brown to black, brittle...combustible rock containing more than fifty percent by weight and more than seventy percent by volume of carbonaceous material..." (Mitchell,1985). Two varieties (VI-VII) qualify as bastard coals (Mitchell,1985), meaning any coal with a high clay content. Two are classified as either lignite or subbituminous coal (VIII-IX). The facies are numbered from I to IX with a higher number indicating increased organic carbon content.

Facies IA (Figure 5) is a semi-waxy, moderately laminated to blocky, light gray (N7) shale with no carbonaceous flecks. Yellow mottling is evident in places, and the silt content is high, usually as lenses that define the lamination in the shale. Concretions of hematite are common on both macroscopic and microscopic levels. The kaolinite content is variable, ranging from 17 to 47 (see Clays and Total Organic Carbon chapter, 'Methods). Organic content is low, usually below 5 percent, with a few samples as high as 9.5 percent.

Figure 5. Facies IA shale (2X actual size; (Sample #13B). Notice lamination marked by silt lenses.

Facies IB is similar to facies IA, but laminations are absent. Silt is present in higher amounts, but is evenly distributed throughout the shale. Hematite is rare, occurring as poorly developed scattered microscopic concretions.

Facies II (Figure 6) is a waxy, crudely laminated to blocky, medium dark gray (N 4) shale with little or no carbonaceous flecks. Rare silt lenses occur parallel to the lamination. Kaolinite averages around 20, and the organic content is approximately 10 percent.

Facies III (Figure 6) is a semi-waxy, friable, crudely laminated, light olive gray (5 Y 6/1) shale with abundant carbonaceous flecks. It is marked by a high kaolinite content of around 70, and an organic carbon content between 10 and 20 percent.

Facies IV (Figure 7) is a semi-waxy, crudely laminated, pale yellowish brown (10 YR 6/2) shale with rare plant impressions on lamination planes. There are rare silt lenses parallel to the lamination. This facies is normally closely associated with lignite.

Facies V (Figure 7) is a waxy, crudely laminated, brownish black (5 YR 2/1) carbonaceous shale with visible carbonaceous flecks present, and occasional slickensides. The kaolinite content ranges from 15 to 25, and the total organic content varies from 25 to 45 percent.

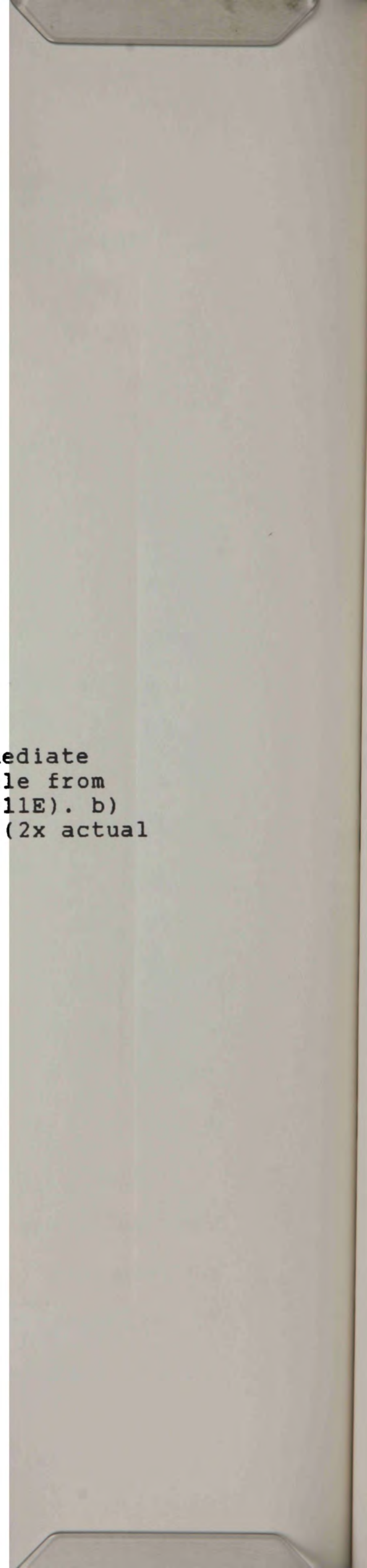

Figure 6. Typical shale facies with intermediate organic carbon content. a) Facies II shale from lower shale member (actual size; Sample #11E). b) Facies III shale from lower shale member (2x actual size; Sample #13M).

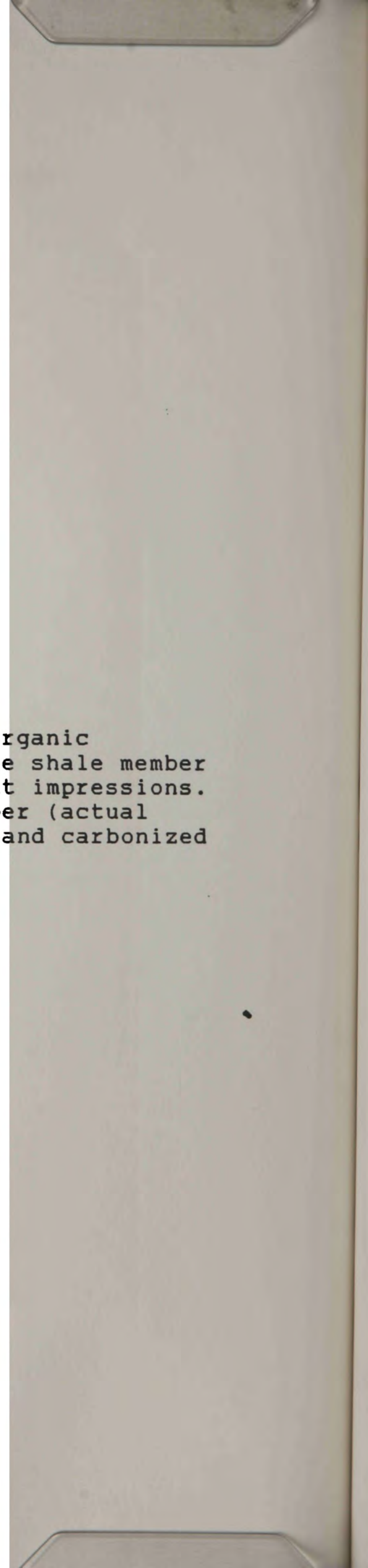

Figure 7. Shale facies with increasing organic content. a) Facies IV shale from middle shale member (actual size; Sample 22F). Notice plant impressions. b) Facies V shale from lower shale member (actual size; Sample 11F). Notice waxy luster and carbonized stem.

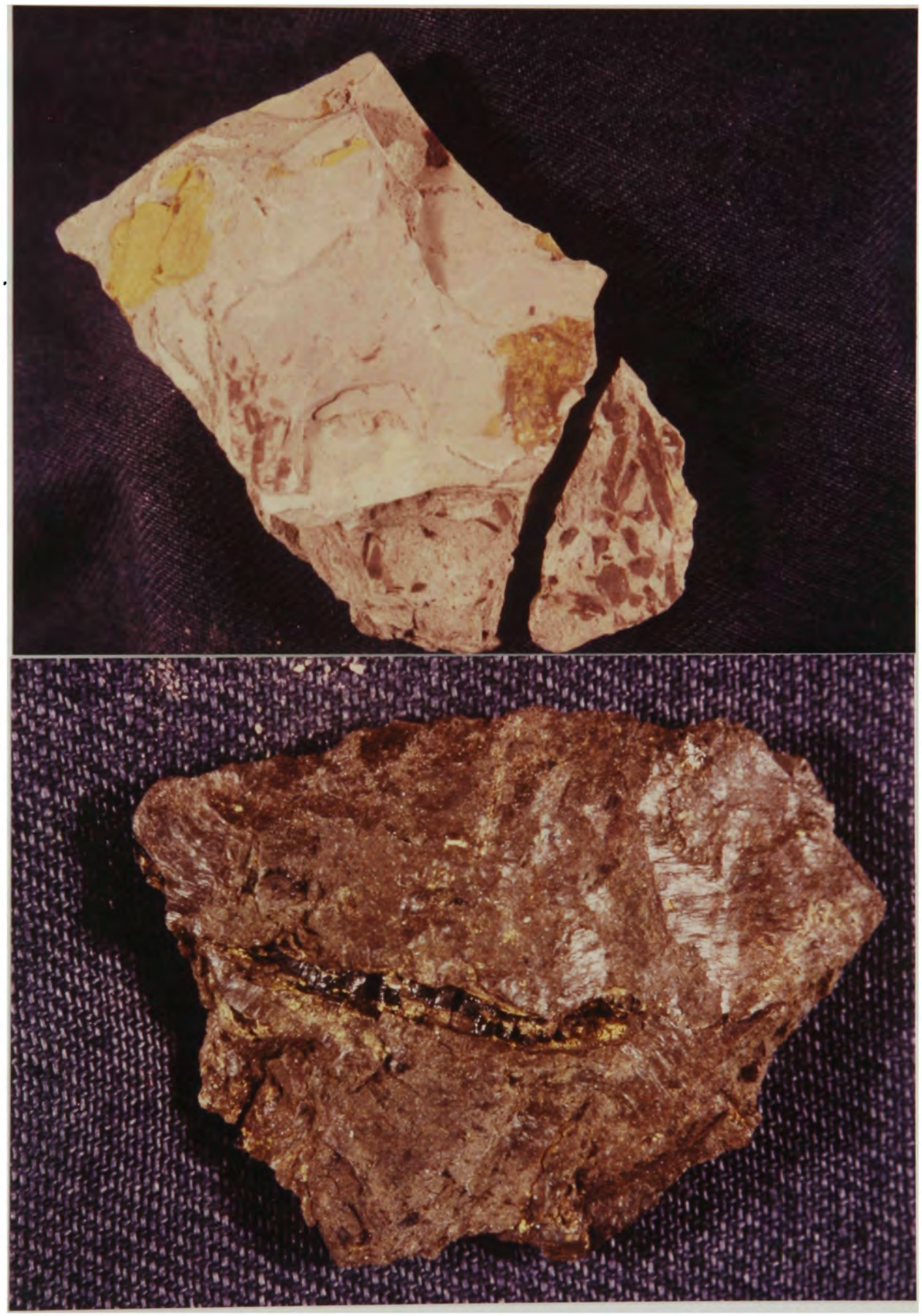

Facies VI contains 70 percent organic carbon, with the remainder clay minerals and detrital grains. This facies is described here as "lignitic clay" (Figure 8). It is characterized by a pale yellow gray (5 Y 8/1) and dark gray (N 3) mottled appearance with abundant visible organic material, a kaolinite value of 100, and well developed fissility.

Facies VII is a second variety of clay-rich lignite (Figure 9). This is brownish black (5 YR 2/1) lignite with intimately mixed waxy clay of the same color. These lignites are very friable and show well developed fissility.

Facies VIII is a true lignite (Figure 9). It is very friable, fissile, brownish black (5 YR 2/1) and has a minor clay fraction.

Facies IX is a subbituminous coal (Figure 10), intermediate in grade between lignite and bituminous coal. It is blockier than the other facies and has poorly developed fissility. It is darker (N 1) than the other units, and shiny on freshly broken surfaces.

Summary

It is possible to define facies in the shales and lignites of the lower shale and middle shale members of the Aguja Formation based on kaolinite content (see Clays and Total Organic Carbon chapter), organic carbon content

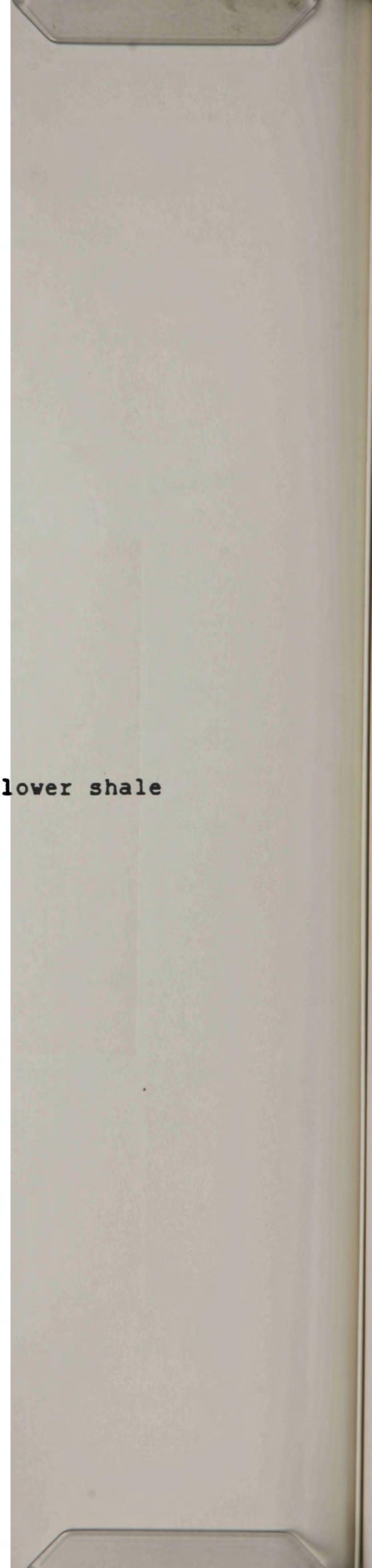

Figure 8. Facies VI "lignitic clay" from lower shale member (2X actual size; Sample #13C).

Figure 9. Organic carbon-rich facies. a) Facies VII "clayey lignite" (2X actual; Sample #11C). b) Facies VIII lignite from lower shale member (actual size; Sample #15).

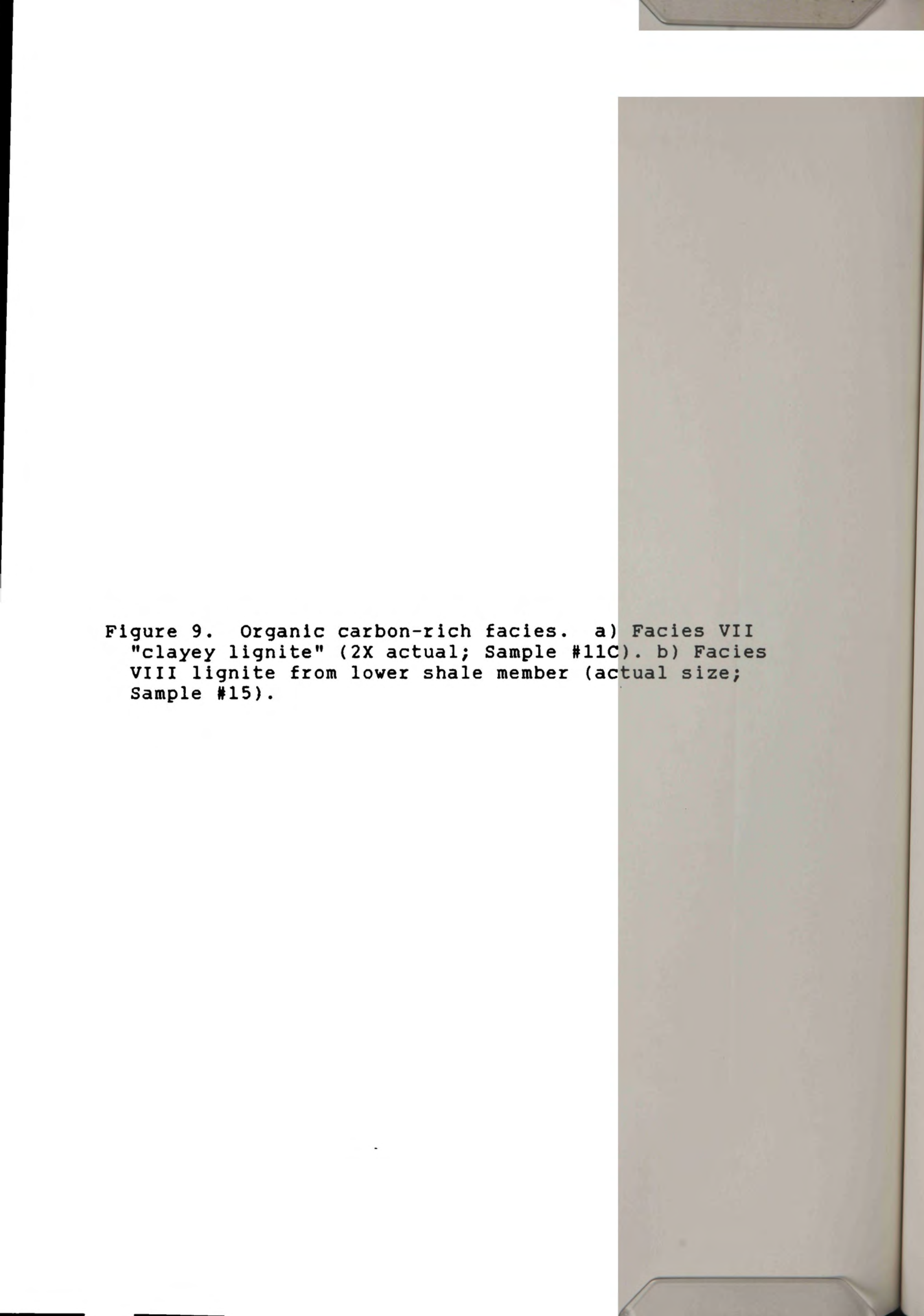

Figure 9. Organic carbon-rich facies. a) Facies VII "clayey lignite" (2X actual; Sample #11C). b) Facies VIII lignite from lower shale member (actual size; Sample #15).

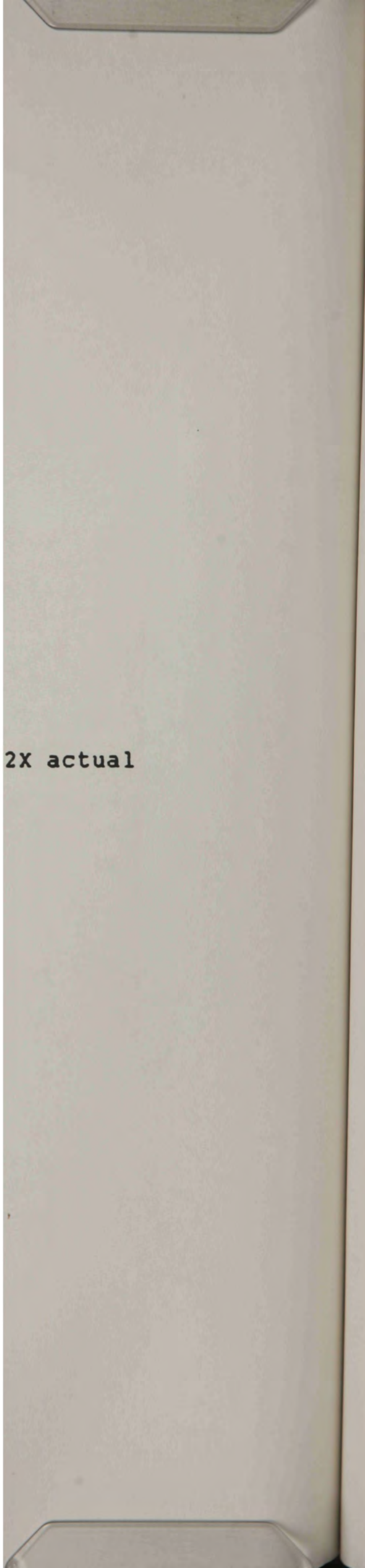

Figure 10. Facies IX subbituminous coal (2X actual size). Notice the luster.

(see Clays and Total Organic Carbon chapter), degree of lamination, silt content, luster, and color. The facies range from "clean" light gray shale (facies I) with low organic carbon and kaolinite content to subbituminous coal (facies IX). The facies alternate to yield a crude cyclicity in the section, defined by variations in the clay and total organic carbon content.

CHAPTER III

PETROGRAPHY

Examples of each of the various shales, lignites, and interbedded sandstones were examined petrographically. This allowed identification of mineral and organic phases present. In addition to several clay mineral types, the shale components consist of silt-sized detrital grains, iron oxides, and various organic maceral types, and several clay minerals. These components have varying detrital and authigenic origins.

Methods

Sandstone samples were impregnated with epoxy to stabilize friable grains prior to being thin-sectioned. Argillaceous samples, that were too fine-grained to accept the epoxy, were dried in an oven, and coated in epoxy to protect them from water during the cutting process. Samples were sawed perpendicular to bedding and ground to a smooth flat surface using carbide sandpaper. They were then cut into blanks for thin sectioning. Some samples did not survive the epoxy-impregnation and sawing procedure due swelling of the smectite clay in the cooling water. The samples were analyzed using a standard petrographic microscope. In addition, some samples were

analyzed with fluorescent light to identify organic macerals in the carbonaceous shales.

Petrographic Analysis

Clay Fraction

The clay in the shales is very uniform in appearance and exhibits varying degrees of preferred orientation. Clay orientation is reflected by uniform extinction of the clay fraction, or "birefringence fabric" (Figure 11). This fabric becomes more pronounced with increasing clay orientation (Williams et al., 1982). Strongly oriented samples do not belong to any particular facies, but many of the facies IA shales show moderate to good orientation. As no pedogenic fabric is evident in the clay matrix, orientation is probably due to depositional or compactional causes.

The bulk of the clay is identified as smectite, based on its birefringence and index of refraction. The smectite is clearly of detrital origin, demonstrated by intimate mixing with silt-sized detrital grains and organic material. There are no "pure" smectite layers or relict shard textures that might be expected if the smectite were derived from alteration of volcanic ash airfall.

Figure 11. Birefringence fabric (uniform extinction) of clay particles in facies III shale (upper and lower figures). Field of view 5mm. Crossed polarizers (Sample #22A).

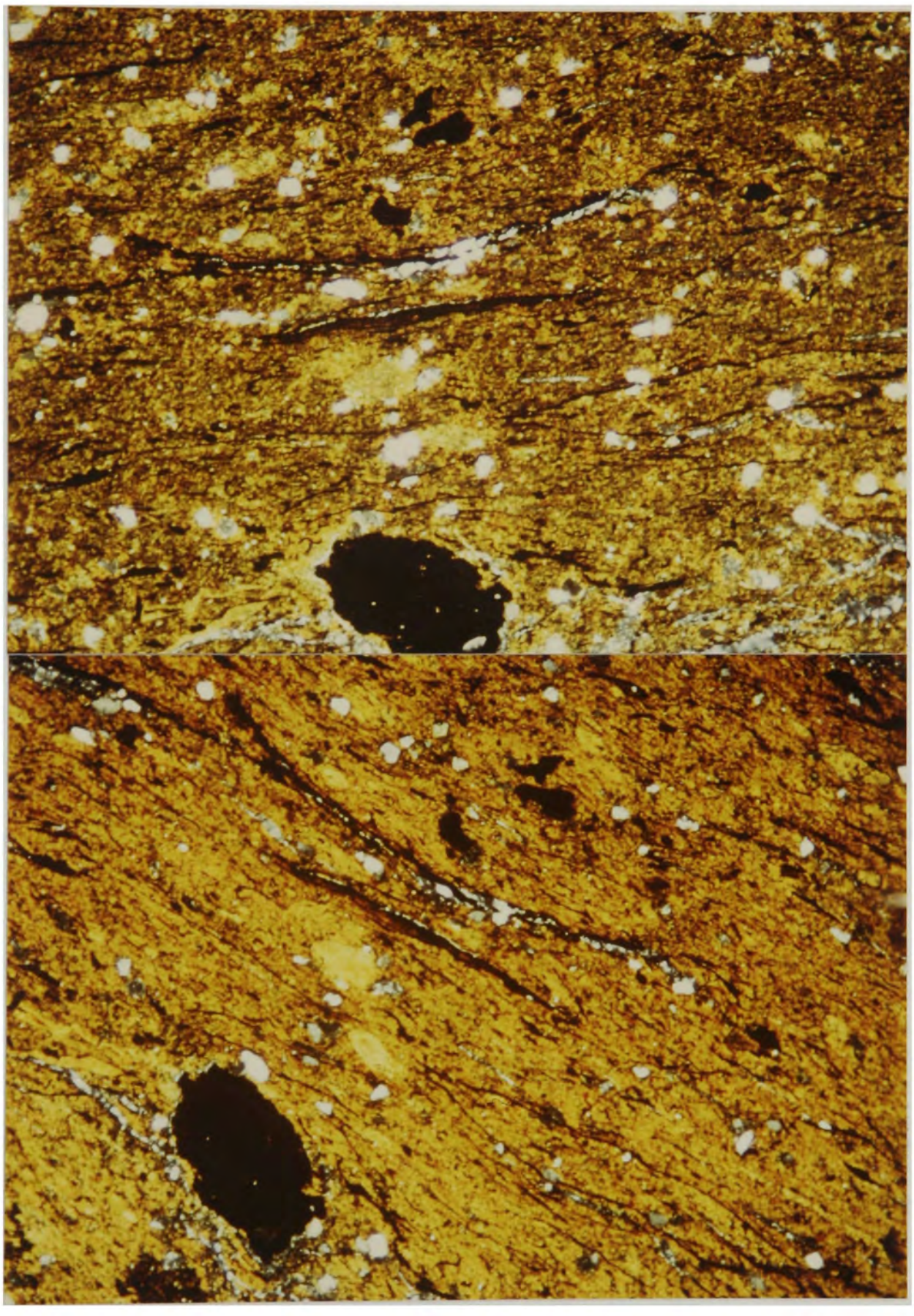

Kaolinite is visible in several samples as low birefringent "splotches" with diffuse boundaries within the higher birefringent smectite. The kaolinite is clear in plane polarized light, whereas the smectite is normally yellow stained, probably from interaction with iron oxides and/or organic matter. Kaolinite is also found as a pore-filling cement in the silt-sized lenses within the shale, and as patchy cement in the sand beds associated with the shales. Accurate identification is complicated in some shales where kaolinite is more intimately mixed with the smectite. Although it is not clear what controls the location and presence of the kaolinite, it appears to be authigenic in origin in most cases. Illite is present in the shales, but is not readily identifiable in thin section. Muscovite is present in minor amounts, and may be identified as illite on the X-ray diffraction readout as it shares a peak with illite (see Clays and Total Organic Carbon chapter). Chlorite is present as light green (plane polarized light) "clasts" of probable detrital origin.

Fractures are common in the shales (Figure 12). Greater numbers of fractures and more irregular fractures are found in shales with higher organic content. Many fractures contain patches of lath-like gypsum crystals. The gypsum is mostly restricted to patchy areas of fracture fill; however, in some areas gypsum fills

Figure 12. Fractures oriented parallel to lamination in a facies V shale. Field of view 5mm. Plane light. (Sample #23A).

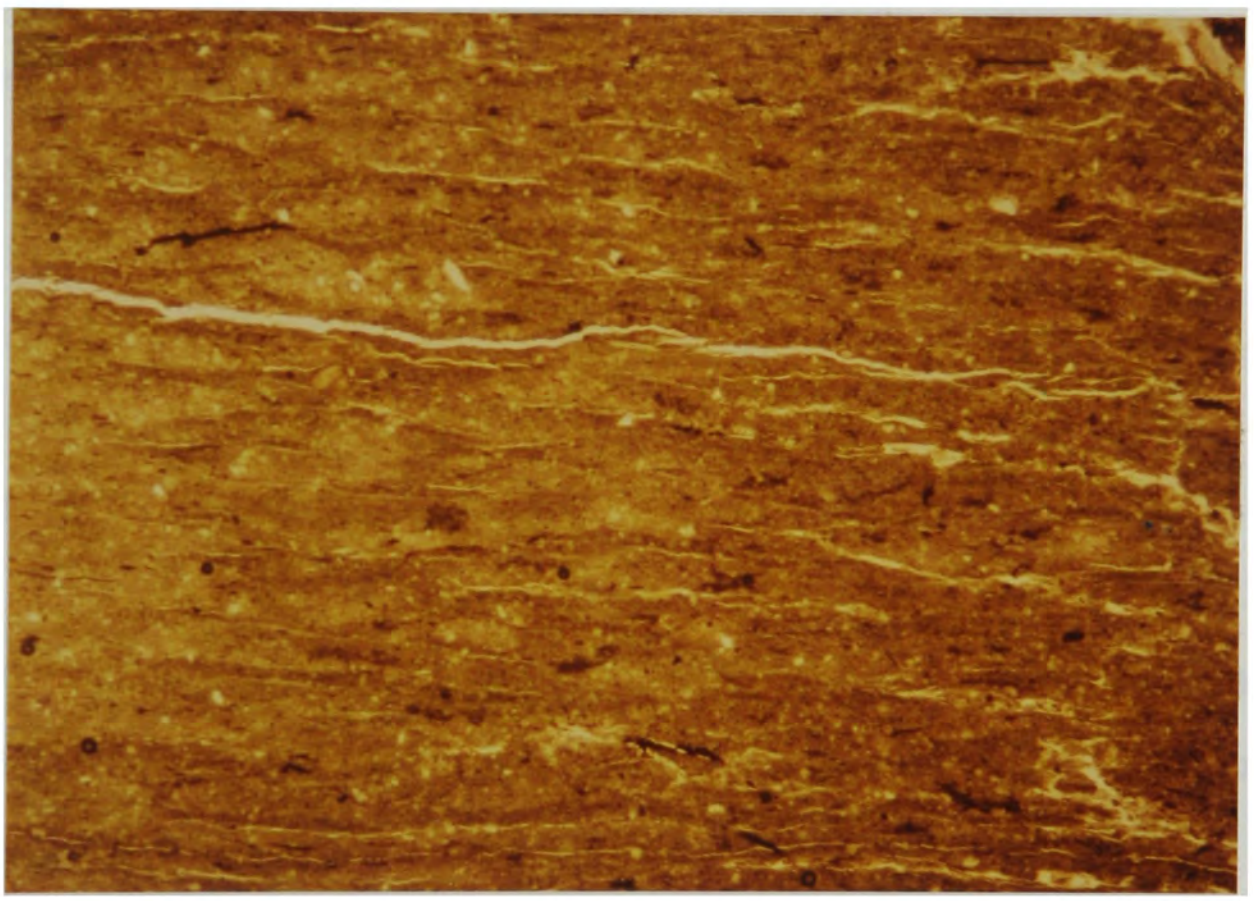

unidentified voids in the shale. The fractures are relatively recent features, and the gypsum is clearly authigenic. Fracture patterns are more random in higher rank coals than in the carbonaceous shales.

Silt Fraction

The shales contain a varied amount of silt-sized material, as well as a minor sand content. Quartz, plagioclase, chert, and various other grains are present in many samples. These grains are detrital in origin, and range from well-rounded to angular, indicating varied transport histories. The grains occur in discrete lenses in the shale (Figure 13a), or randomly scattered throughout (Figure 13b). The boundaries of the silt lenses with the surrounding clay range from sharp to diffuse. Some appear to be burrow or root-mold fillings. The lenses are most common in facies I through V, but are also found in the carbonaceous facies.

Zircon is another silt-sized component of the shales. It is found in most of the samples, but is a minor constituent. Zircon occurs as angular broken fragments and euhedral crystals exhibiting prismatic habit (Figure 14). The zircon ranges from clear to lilac in plain light. Alkali feldspar grains with a euhedral to subhedral outline are also found (Figure 15). These crystals are rectangular, lack twinning, and show minor

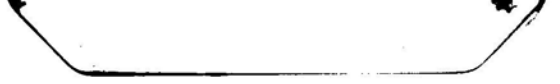

Figure 13. Shale with typical silt and sand-sized constituents a) in a lense (burrow fill ?) of facies IA shale. Field of view 5mm. Crossed polarizers. (Sample #13J). b) randomly scattered in facies IB shale. Field of view 5mm. Crossed polarizers. (Sample #29A). Notice burrow(?) on the right.

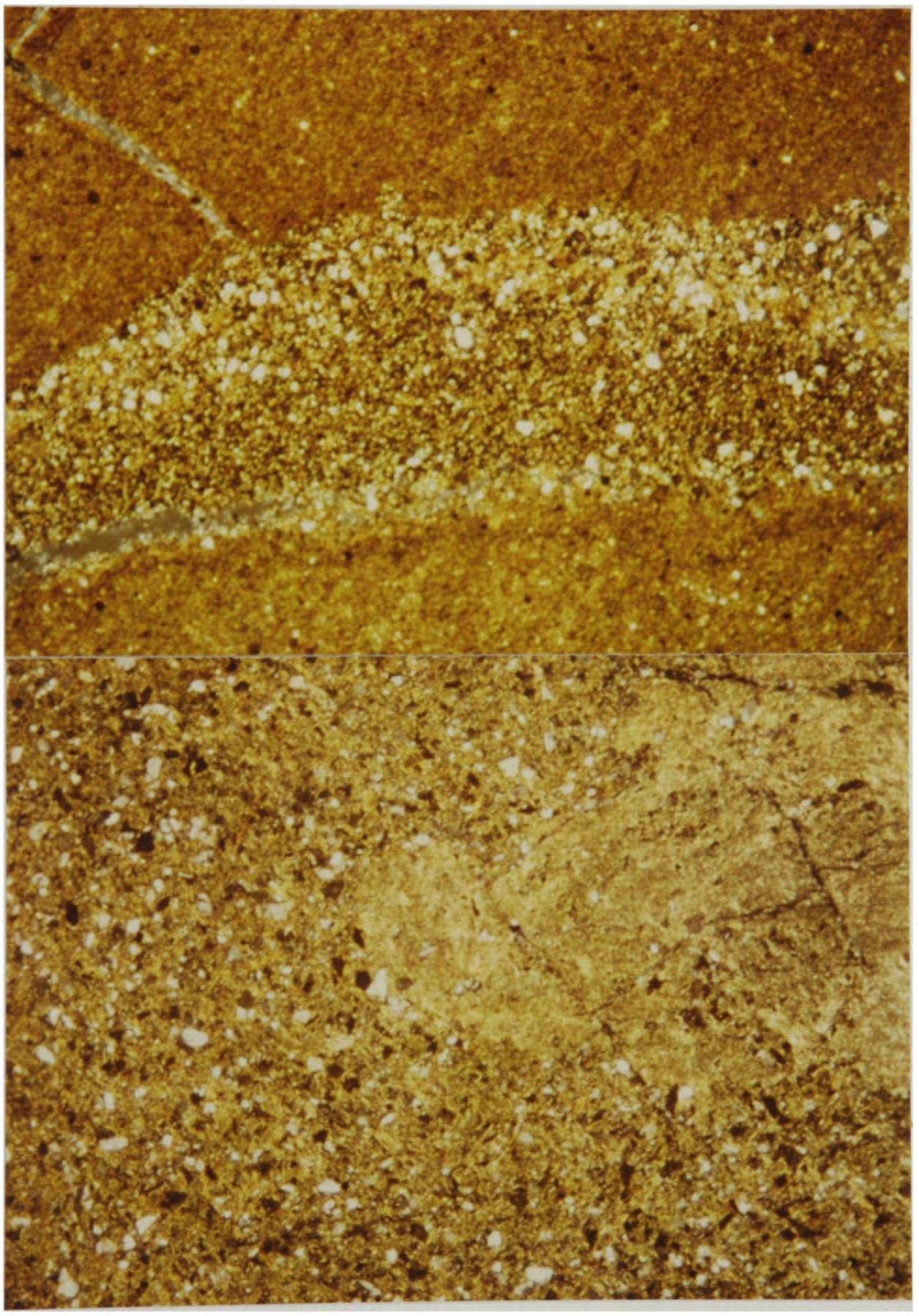

Figure 14. Euhedral zircon crystal (Sample #13J) in a facies IA shale silt lense in a) plane light b) Crossed polarizers. Field of view in both 0.5mm.

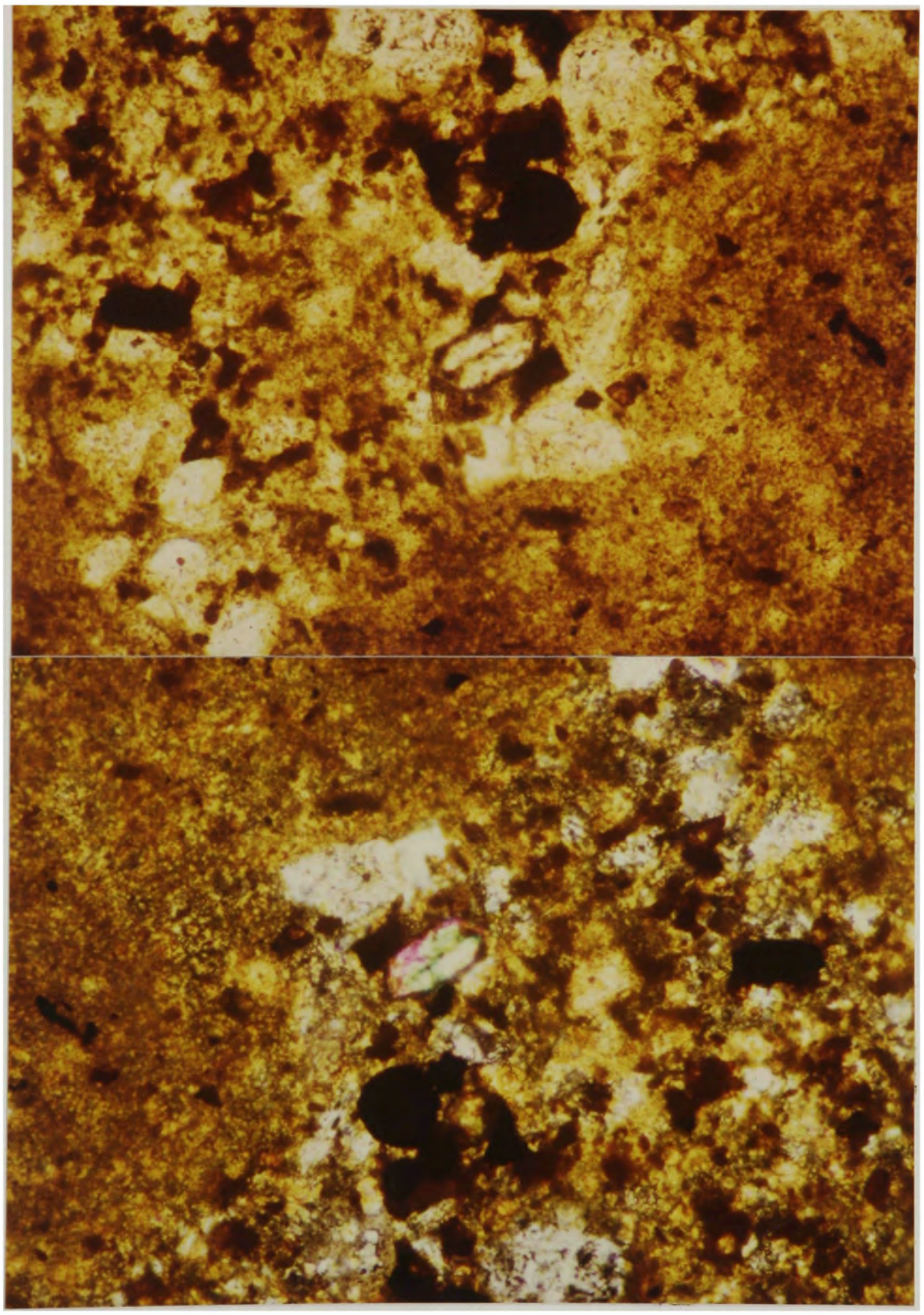

Figure 15. Alkali feldspar crystal in facies VII "clayey lignite." Field of view 0.5mm. Crossed polarizers. (Sample #11C). Carbonaceous smectite is to the left, and epoxy is on the right.

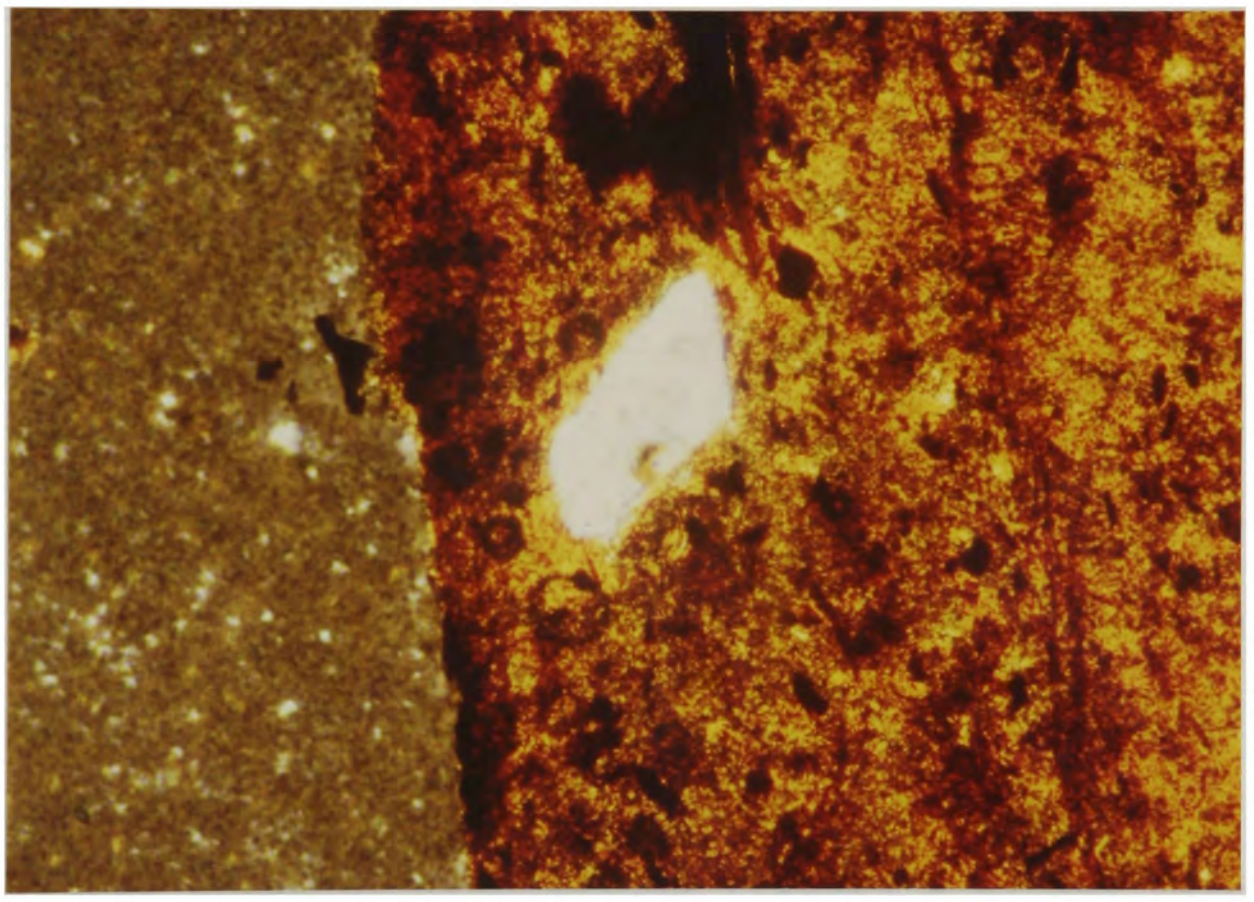

Figure 16. Two forms of crystalline iron oxide in the shales. a) Hematite concretion in a facies IA shale displaying wormy texture on the boundaries. Field of view 0.25mm. Plane light. (Sample #13B). b) Isolated euhedral to subhedral authigenic hematite crystals in facies V shale. Field of view 0.25mm. Plane light. (Sample #11A).

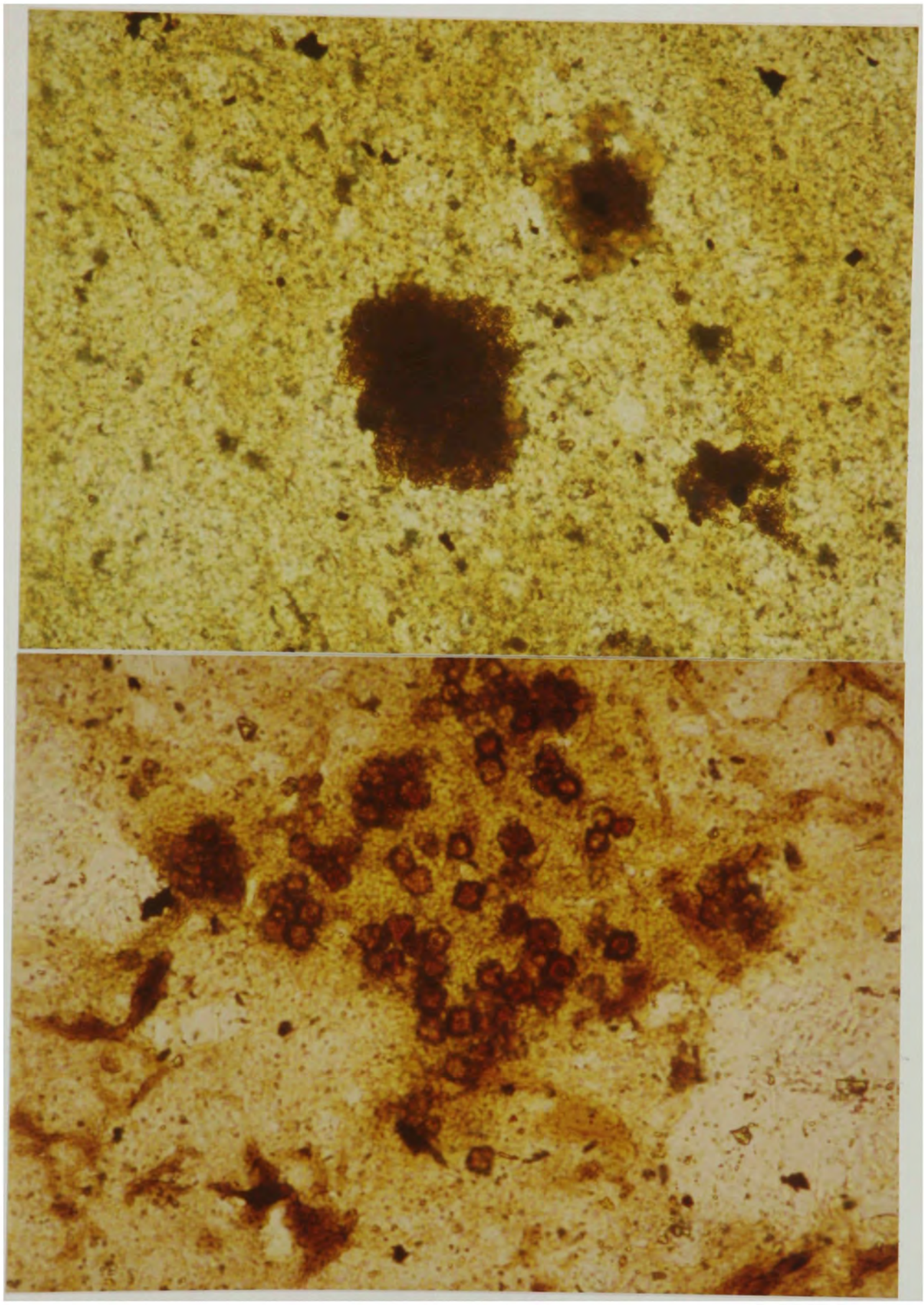

Figure 17. Zones of iron oxide concentration. a) Zones of iron oxide concentration in facies IV shale. Field of view 5mm. Crossed polarizers. (Sample #22E). b) Iron oxide hardened zone with crack propagating around it in facies IV shale. Field of view 1mm. Plane light. (Sample #22E).

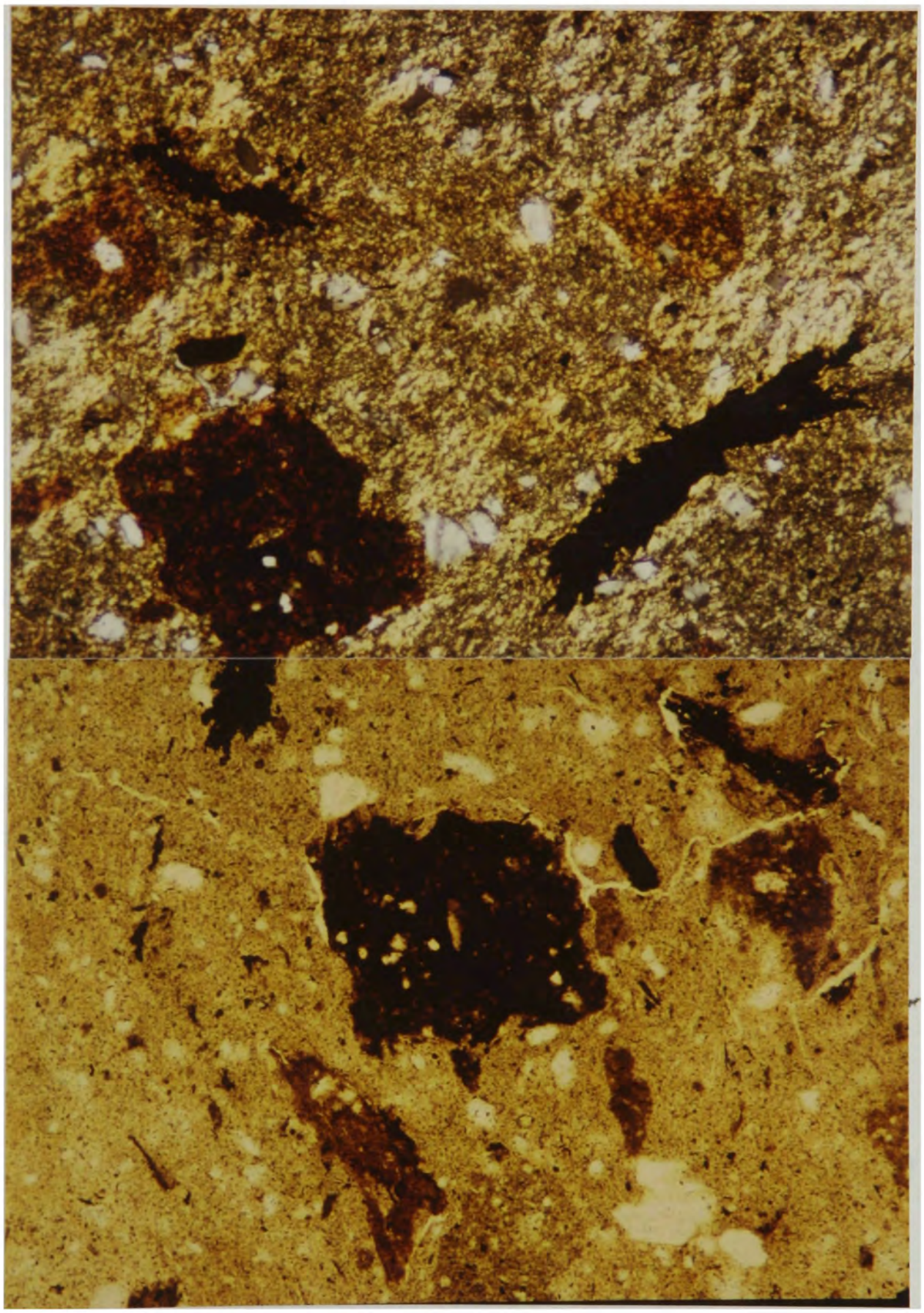

iron oxides are preferentially excluded (Figure 18). Such zones may also be related to some chemical diagenetic process. These zones are marked by less of the brown stain common to most of the clay.

An unusual textural feature is present in some of the very carbonaceous shales. The samples exhibit a light "imprinted" wormy texture on the shale, similar to that observed around the edges of the hematite concretions. The texture is normally seen around organic macerals, but is also seen as a general feature common across the sample. This is similar in appearance to goethite-organic complexes described by Schwertmann and Taylor (1977). Such compounds occur where ferrous iron is put in solution by reaction with organic compounds, and forms an iron-organic complex.

Calcite occurs as small (less than 1.5mm in dia.) concretions (Figure 19) or as scattered crystals. The concretions are roughly oval, and exhibit a patchy or wormy texture. Calcite is found in the cycle C-C' mentioned before (see Clays and Total Organic Carbon chapter), and in facies IA shales. Calcite concretions are not as widespread as iron concretions, and are observed in the lower shale and upper shale.

Siderite occurs as a cement and as concretions (less than 1 mm) in several samples, and exhibits two different crystal morphologies. Where siderite occurs as cement in

Figure 18. Zones where iron concretions (black spots - probably pseudomorphic after pyrite) are preferentially excluded in facies IA shale. Field of view 5mm. Plane light. (Sample #13B).

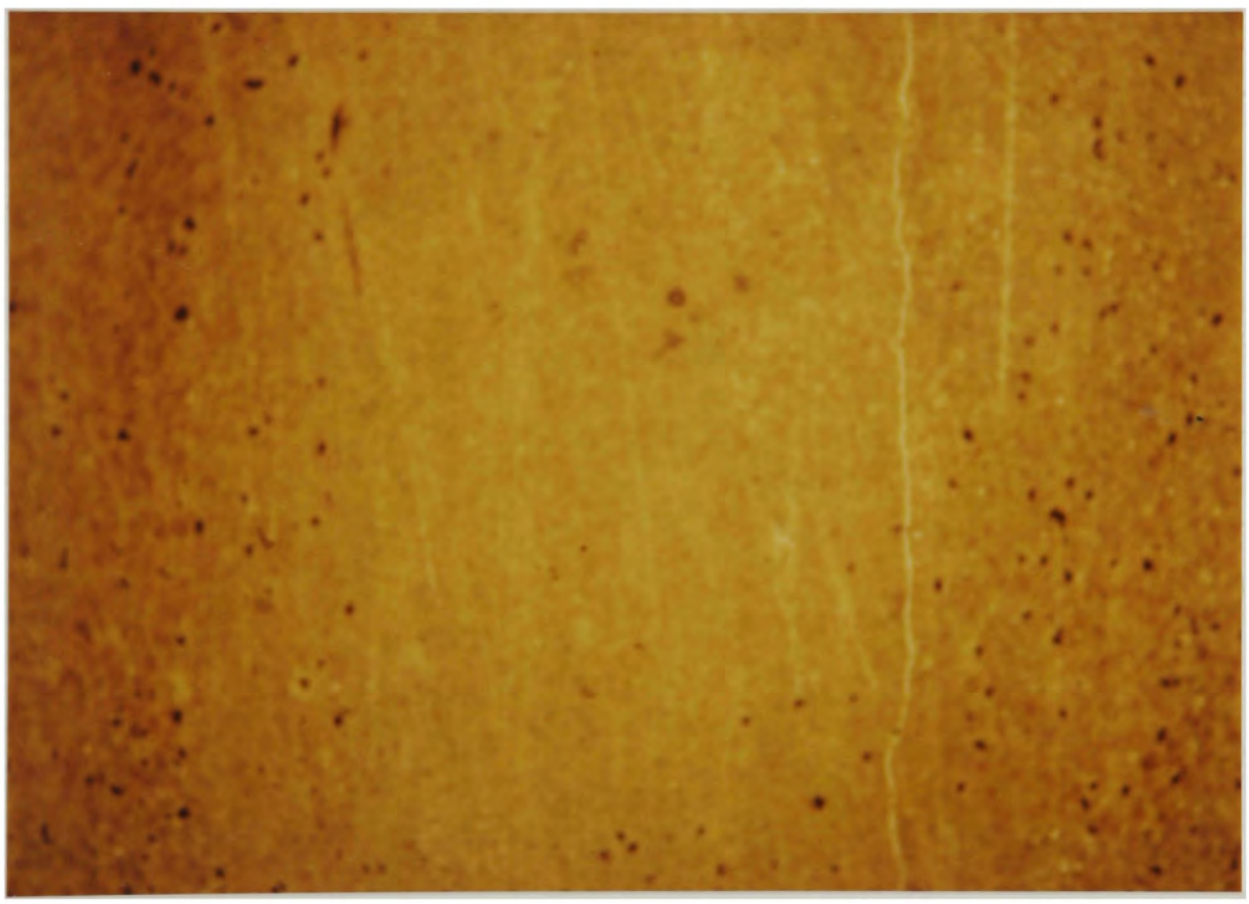

Figure 19. Calcite concretion in facies III shale displaying wormy texture. Field of view 1mm. Crossed polarizers. (Sample #13M).

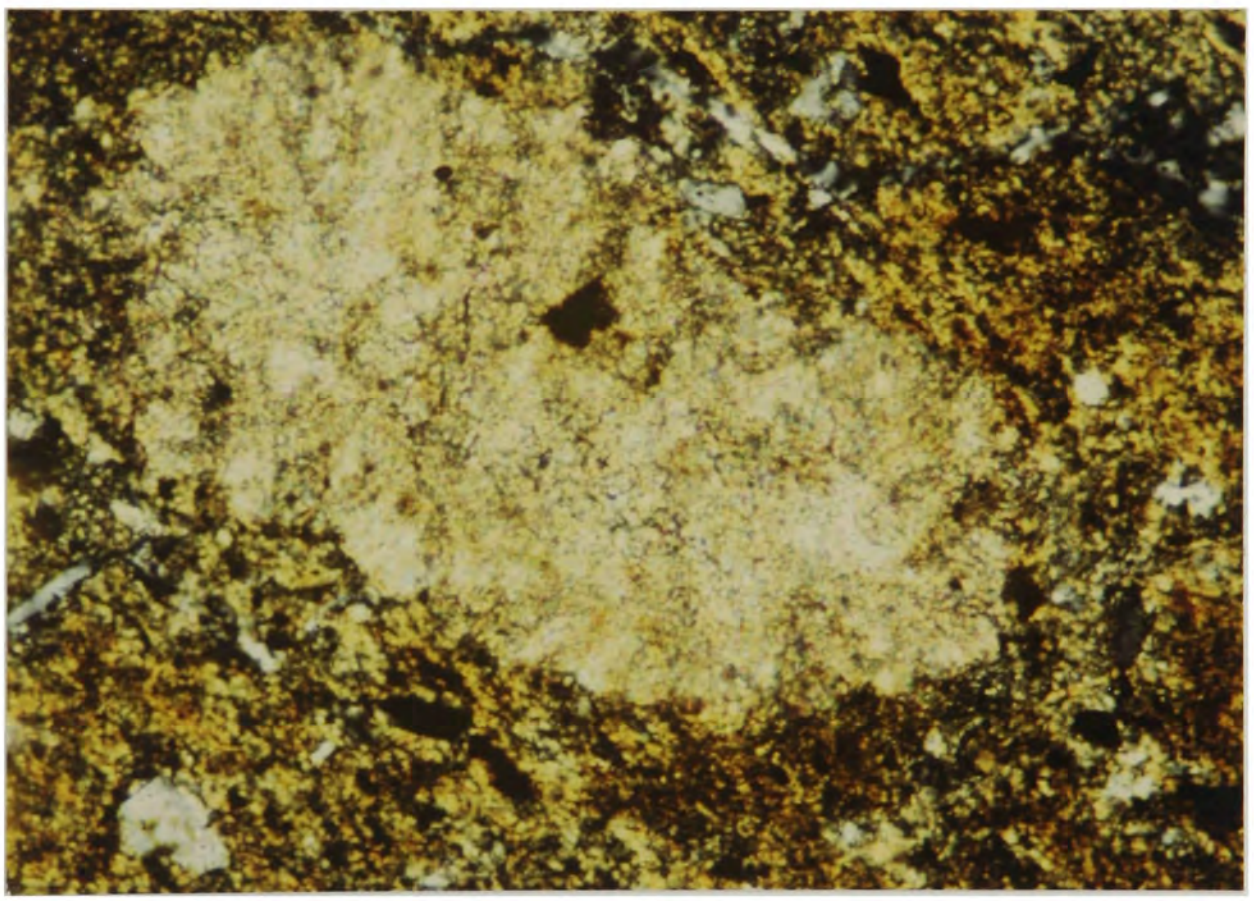

sandstone, the crystals are well formed, exhibiting a euhedral rhombic habit and high relief. The crystals are pale green to clear with a brown stain in plane light (Figure 20a). Siderite also occurs as concretions (Figure 20b) and cement in some shales. Its appearance in plane light is similar to that in sandstone, but the crystal shapes are less developed, exhibiting subhedral to anhedral form. Siderite occurs in shale fractures as lens-shaped bodies or as round concretions in the matrix.

Organic Material

The carbonaceous material found in the shales ranges from very fine, diffuse light yellow-brown particles to large opaque woody fragments. In several of the organic-rich shales various organic macerals are laminated in alternating bands of yellow and dark brown (Figure 21a). The dark laminations are composed of fragments of unidentifiable opaque angular woody material or roughly ovoid (stem?) fragments (Figure 21b). Scattered throughout most of the samples are small unidentifiable opaque and angular flecks of carbonaceous material.

The carbonceous shales of the section were analyzed under fluorescent light to identify the organics present. A carbonaceous shale from the base of the upper shale member (Figure 21a) reveals cutinite, which is derived from leafy material. It is seen in Figure 21a as the

Figure 20. Two examples of siderite crystals in sandstone and shale. a) Euhedral siderite crystals as cement in lower shale sandstone. Field of view 0.5mm. Crossed polarizers. (Sample #10). b) Siderite concretions in a facies V shale. Field of view 1mm. Plane light. (Sample #11B).

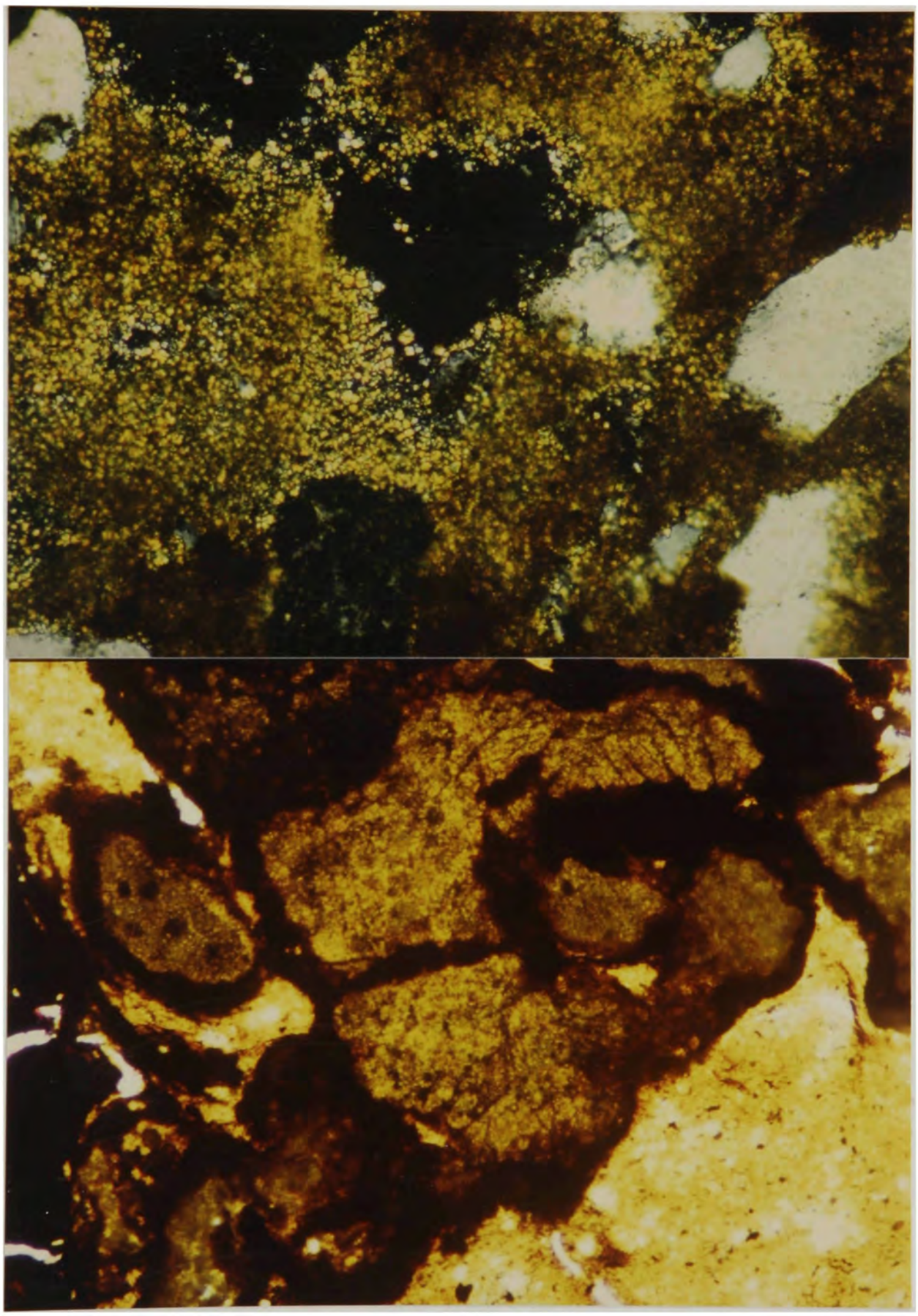

Figure 21. Two forms of organic matter from organic rich shales. a) Laminated organic matter in a facies VII "clayey lignite." Field of view 5mm. Crossed polarizers (Sample #23B). b) Low grade woody fragments in a facies III shale. Field of view 5mm. Crossed polarizers. (Sample #22A). Notice ovoid crushed stem (?) in center.

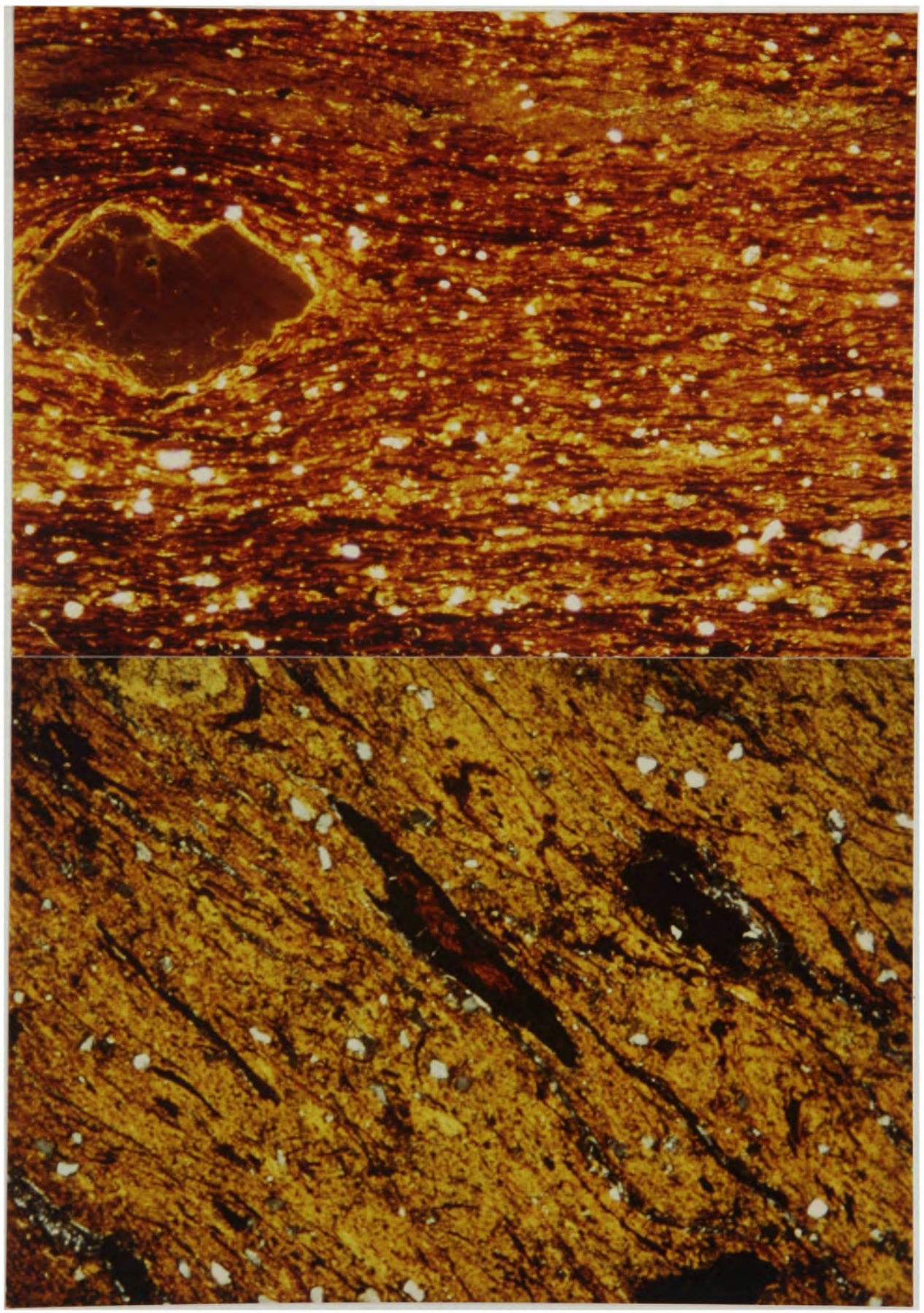

roughly parallel dark bands. Pseudovitrinite, which is an organic maceral derived from low grade woody material, is found in several samples from the lower shale.

Sandstones

The sandstones of the section are all similar in detrital framework grain composition. Quartz, plagioclase (with albite twinning), and chert comprise the bulk of the grains. Zircon, microcline, and opaque heavy minerals are accessory minerals. All the detrital material is fine sand size, except for zircon which is silt-sized. The majority of the sandstones are cemented by blocky equant calcite and patchy kaolinite (Figure 22a). Exceptions to this are one sandstone in the upper shale that is entirely cemented with blocky equant calcite (Figure 22b), and one above the basal sandstone that is cemented with kaolinite and siderite (Figure 23).

Summary

The shales present here are dominated by smectite with an oriented fabric caused either by depositional or compactional mechanisms. The smectite is probably derived from altered volcanic ash brought to the depositional site by fluvial processes. Kaolinite is present as authigenic low birefringent patches in the smectite. Illite and chlorite are present in minor amounts, but are difficult to identify petrographically.

Figure 22. Two types of cement in sandstone associated with the shales. a) Blocky equant calcite cement in an upper shale member sandstone. Field of view 1mm. Crossed polarizers. (Sample #33). b) Patchy kaolinite and calcite cement in a lower shale member sandstone. Field of view 1mm. Crossed polarizers. (Sample #2mbss).

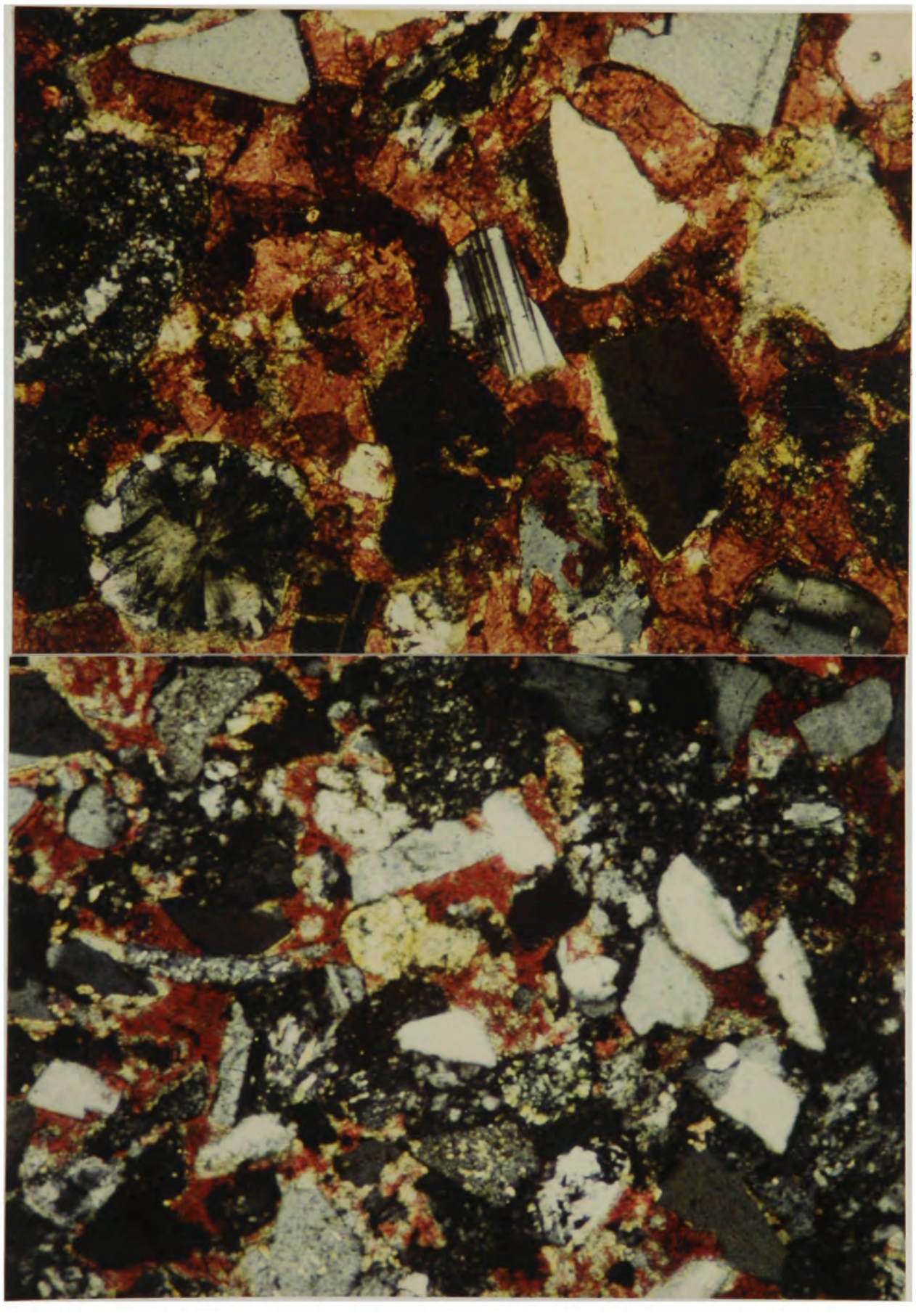

Figure 23. Kaolinite and siderite cemented sandstone in the lower shale member. Field of view 1mm. Crossed polarizers. (Sample #13M).

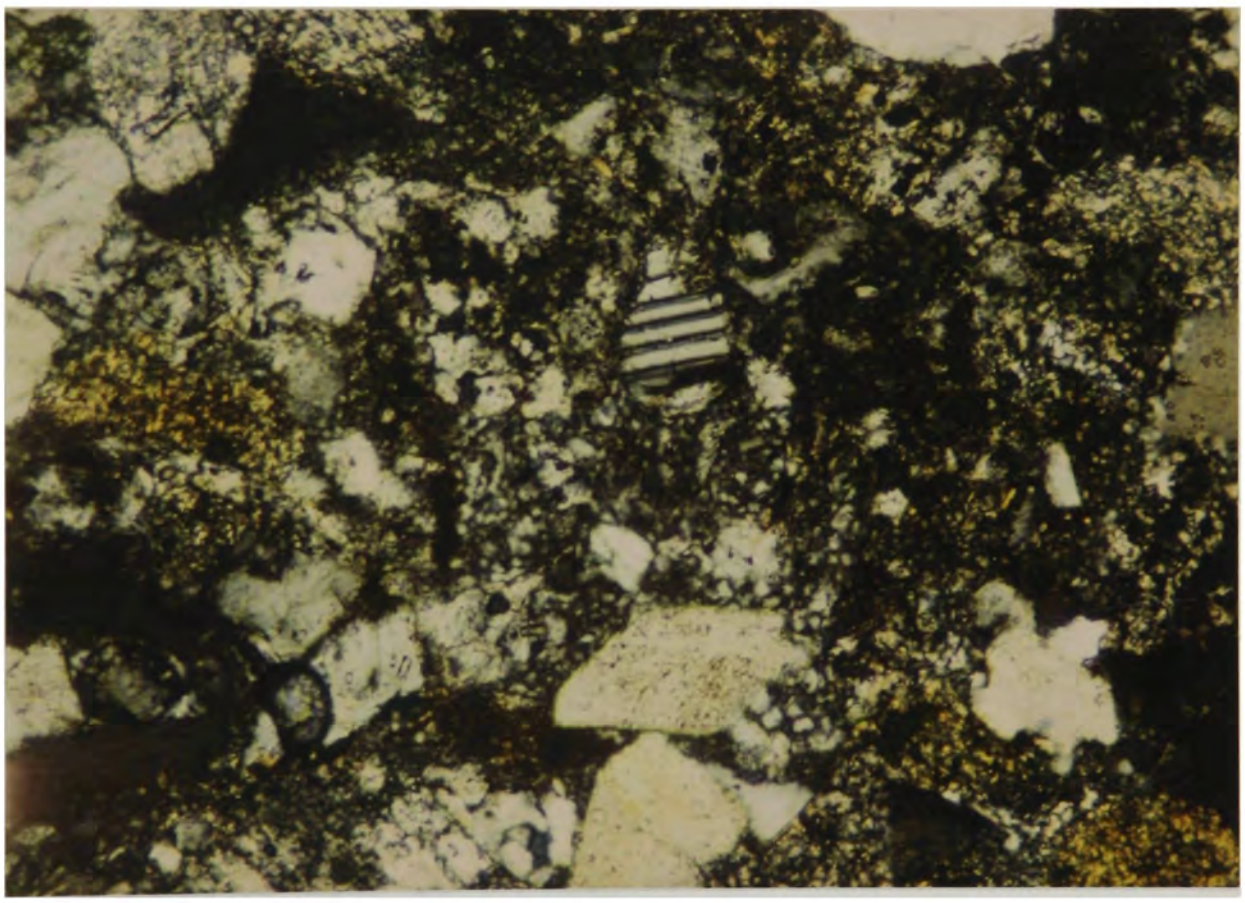

Varying amounts of silt-sized detritus and organic material are present in the shale. The silt-sized material is arranged in lenses or may be randomly scattered, and consists mainly of detrital quartz, chert, and plagioclase. The rounded to subangular nature of the grains indicates varying distances of transport by fluvial processes. Euhedral zircon and alkali feldspar crystals indicate weathering of felsic rocks in the source area or possibly some volcanic ash airfall component in the shale. Gypsum is found as authigenic fracture and void filling. in the samples. The fractures become more numerous and less oriented as organic content increases.

Cement in the sandstones is dominated by blocky equant calcite, with patchy kaolinite and lenses of siderite present. Authigenic concretions of calcite and hematite are present in varying morphologies, and are most prevalent in the facies I shales. Siderite is present as authigenic cement and as concretions in the shales. Authigenic goethite may be present, related to organic complexing with iron. Zones of iron oxide concentration are present in some shales, and appear to harden the clay as concentration increases.

Organic material is varied, ranging from low grade woody material to leaves to organic "stain" complexing with the clay minerals. Occasional hollow oval fragments

of woody material may represent crushed stems. The maceral types present are terrestrial (non-marine) in origin.

CHAPTER IV

CLAYS AND TOTAL ORGANIC CARBON

The clay mineralogy of the section is described in detail in order to determine any differences within or between the shale units. Hand sample analysis, petrography, and X-ray diffraction were employed in order to analyze the clay constituents. The total organic carbon content of the shales was analyzed to describe organic variations between the various shale facies. On the basis of these analyses, relationships between total organic carbon and the clay content are described. It is apparent that kaolinite closely parallels changes in total organic carbon content.

Methods

X-Ray Diffraction

Fifteen samples representative of the various shale facies were selected for study by X-ray diffractometry. The samples were ground with mortar and pestle to obtain the clay-sized fraction less than two microns in diameter. Slides were prepared at room temperature with a relative humidity ranging from 45 to 55 percent. Each sample was examined using a Phillips - Norelco Diffractometer, operating at 40 kilovolts and 20 milliamps with Ni filtered CuK-Alpha radiation. A scanning speed of 2

degrees per minute at ($2^{o}/2\theta$) was used. Bulk mineralogy and mineralogy of the clay fraction were obtained by analyzing bulk random powder samples and oriented aggregate samples of the less than 2 micron fraction. The oriented clay slides were examined again after saturation with ethylene glycol to determine the presence of expandable clay minerals. The relative amounts of the clays, when mentioned in the following text or figures, are given in terms of relative area under the peak in relation to the maximum peak of that clay observed in the samples. For example, if the maximum area observed under the kaolinite peak is 200 cm^2, it is assigned a value of unity and all other kaolinite peaks are described as fractions of that maximum peak (Brindley and Brown, 1980; Brindley and Kurtossy, 1961). These relative clay fraction measurements are only valid for each clay compared from one sample to the next. Comparison of relative area under the peak between clay minerals in any particular sample has no meaning.

The data from X-ray analysis are plotted on Figures 12-14. Clays were not assigned a value for facies VII-IX, as no type sample was analyzed for the lignites.

Total Organic Carbon

Shale samples were prepared for total organic carbon analysis by grinding with a mortar and pestle to obtain an even powder. The samples were then loaded into polyethylene tubes, weighed, and treated with 10 percent HCl (vol./vol.) to remove carbonate. The sample was then diluted with distilled water, centrifuged, and decanted four times to remove the acid. Ten milligrams (carbonaceous shales) or 60 milligrams ("clean" shales) of sample were loaded into 6 millimeter quartz tubes. One gram of CuO and a small strip of silver foil were added to the tubes, which were then evacuated and sealed. The samples were combusted at 800 ^{0}C for 1½ hours, and analyzed on a mass spectrometer (Craig, 1953). The mass spectrometer used was the VG Isogas SIRA 12 with a gas separating system. The total organic carbon content was determined from the partial pressure of CO_2 at the mass spectrometer, after the CO_2 was purified and automatically measured by a Piriani Gauge calibrated with samples that contain known amounts of organic material.

Results and Discussion

Shales throughout the section are dominated by smectite. The shales also contain lesser subequal amounts of kaolinite, illite, and chlorite. The X-ray analysis does not yield exact percentages of the various fractions,

but, based on thin section analysis and diffractometry, a typical shale is composed of about 65 percent smectite, with chlorite, illite, and kaolinite making up less than 10 percent each. The remaining fraction is composed of silt-sized quartz grains, other detrital grains, and organics (see Petrography chapter). These estimates are, however, only a generalization. The percentages vary as the shales become increasingly organic rich, grading to lignite. If the influx of detrital smectite was somehow reduced, or if the shale were free from silt, the relative percentages of silt and organics vary.

Unit Descriptions

Lower Shale Member

The lower shale member is 58 meters thick (Figure 4, Lithology chapter) and is marked by seven distinct lignitic to subbituminous coal units and numerous lignitic stringers. It contains four of the five shale facies, and all four coal facies (see Lithology chapter). There is a crude cyclicity in the shale facies with lignites capping the cycles (Figure 24). The cycles may have various facies ranging from I to V in the lower portion. The shale then generally grades into more organic-rich facies before climaxing with a very organic rich facies corresponding to facies VI-VIII. One occurrence of subbituminous coal was observed very low in the section,

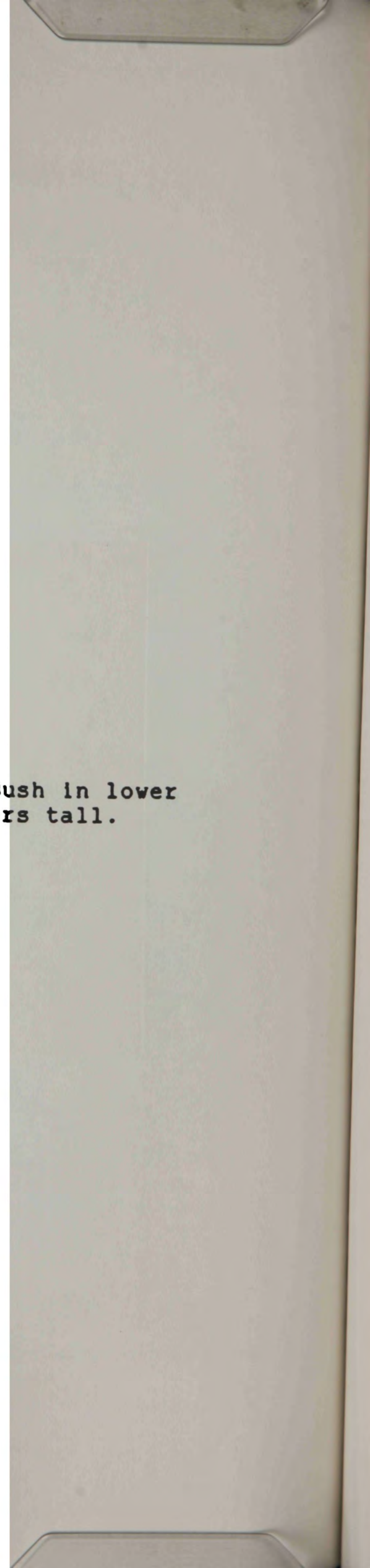

Figure 24. Typical lower shale member. Bush in lower right foreground is approximately 2 meters tall.

but it is associated with (overlies and underlies) sandstone, and not shale. This coal differs from the typical coals of the lower shale, consisting of fine-grained organics, and large pieces of coalified wood.

There are no obvious trends in the smectite or illite clay content (Figure 25) between samples, either in the lower shale or the rest of the section. Both clays seem to fluctuate randomly. The smectite content fluctuates dramatically, while the illite content, in general, remains more stable. The lower illite levels do, however, coincide with peak smectite levels. Kaolinite content parallels or closely precedes increases in the organic content of the shale (Figure 26). Chlorite also follows this trend (Figure 27). It is possible that this results from the fact that chlorite shares the kaolinite peak on the diffractometer readout. Chlorite may therefore be "carried along" artificially with increases and decreases in kaolinite. The inverse is not true, however, because in these samples, kaolinite is the main contributor to the peak, and chlorite is a minor constituent.

Binary plots of kaolinite versus total organic carbon, between the other clays were made to determine if any correlation between clay minerals and total organic carbon could be determined. Only the kaolinite versus total organic carbon plot showed much of a trend, but this was not conclusive. The poor correlation between

Figure 25. Smectite variations plotted versus illite through section A - C' in the lower shale member. Facies relationships depicted below the graph are not to scale.

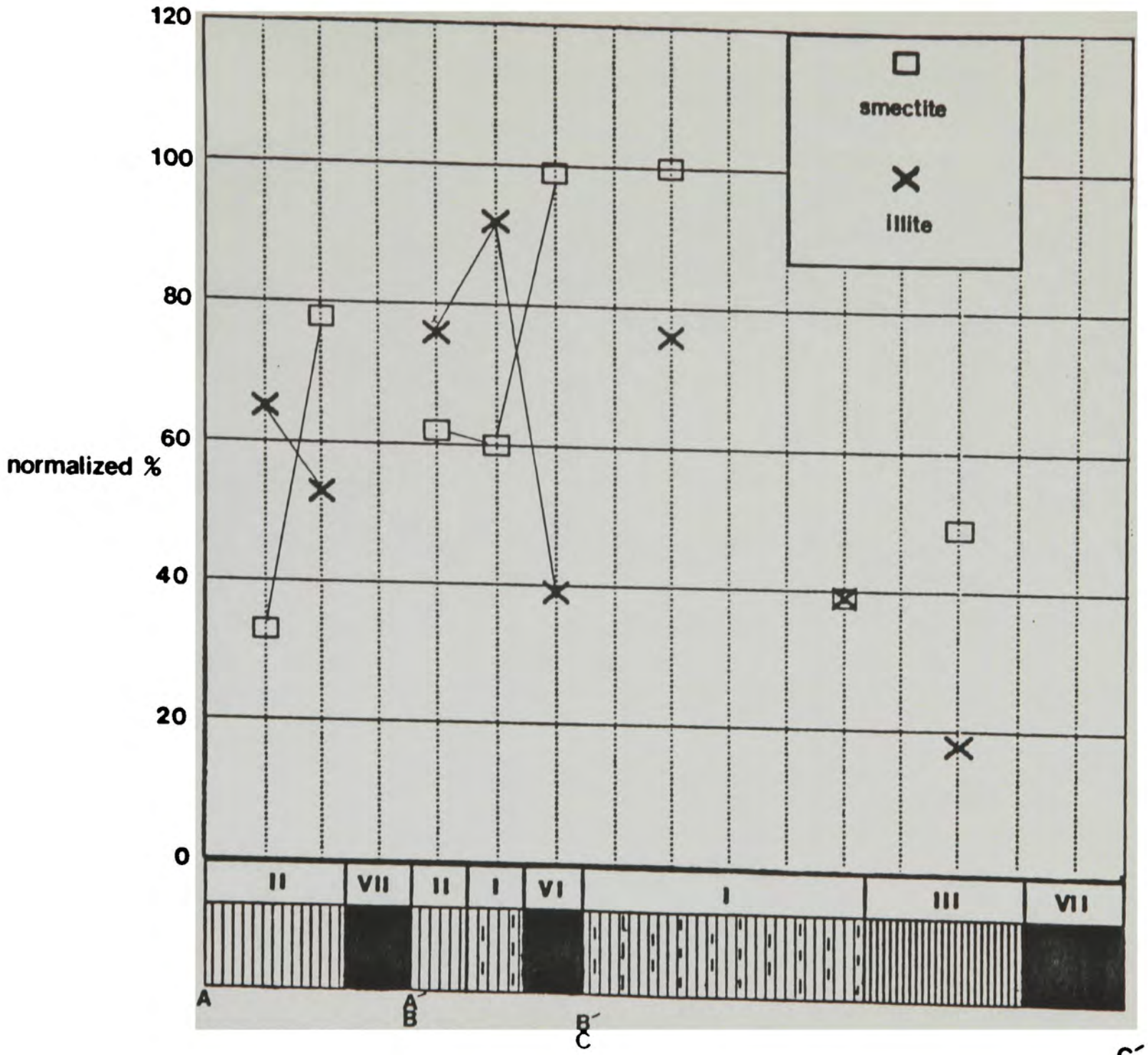
120
100
80
60
40
20
0
normalized %
smectite
illite
II
VII
II
I
VI
I
III
VII
A
A´
B
B´
C
C´

Figure 26. Kaolinite variations with total organic carbon through A - C' in the lower shale member. Facies relationships depicted below the graph are not to scale.

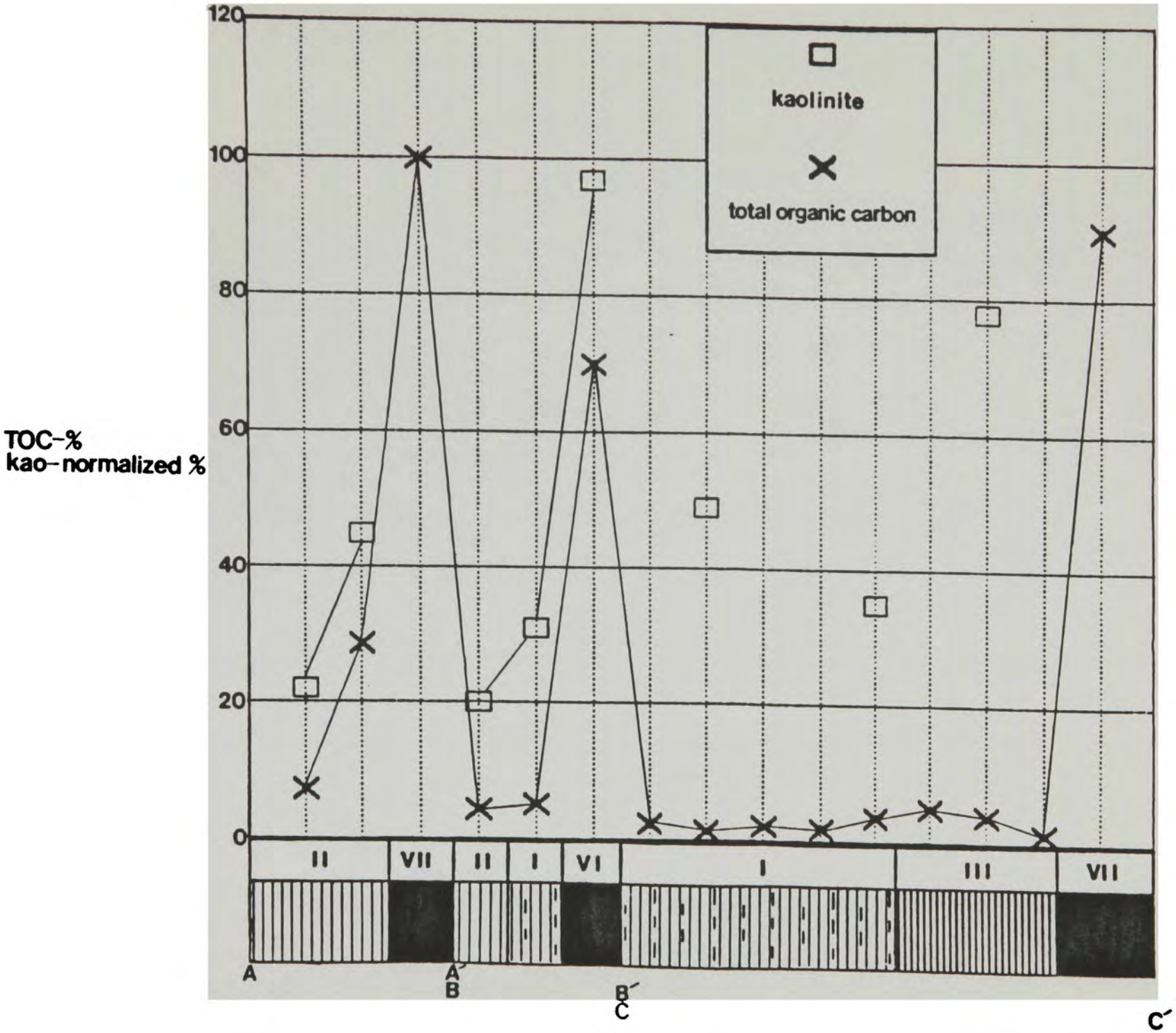
120
100
80
60
40
20
0
kaolinite
total organic carbon
TOC-%
kao-normalized %
II
VII
II
I
VI
I
III
VII
A
A
B
B
C
C'

Figure 27. Chlorite variations with total organic carbon through section A - C' in the lower shale member. Facies relationships depicted below the graph are not to scale.

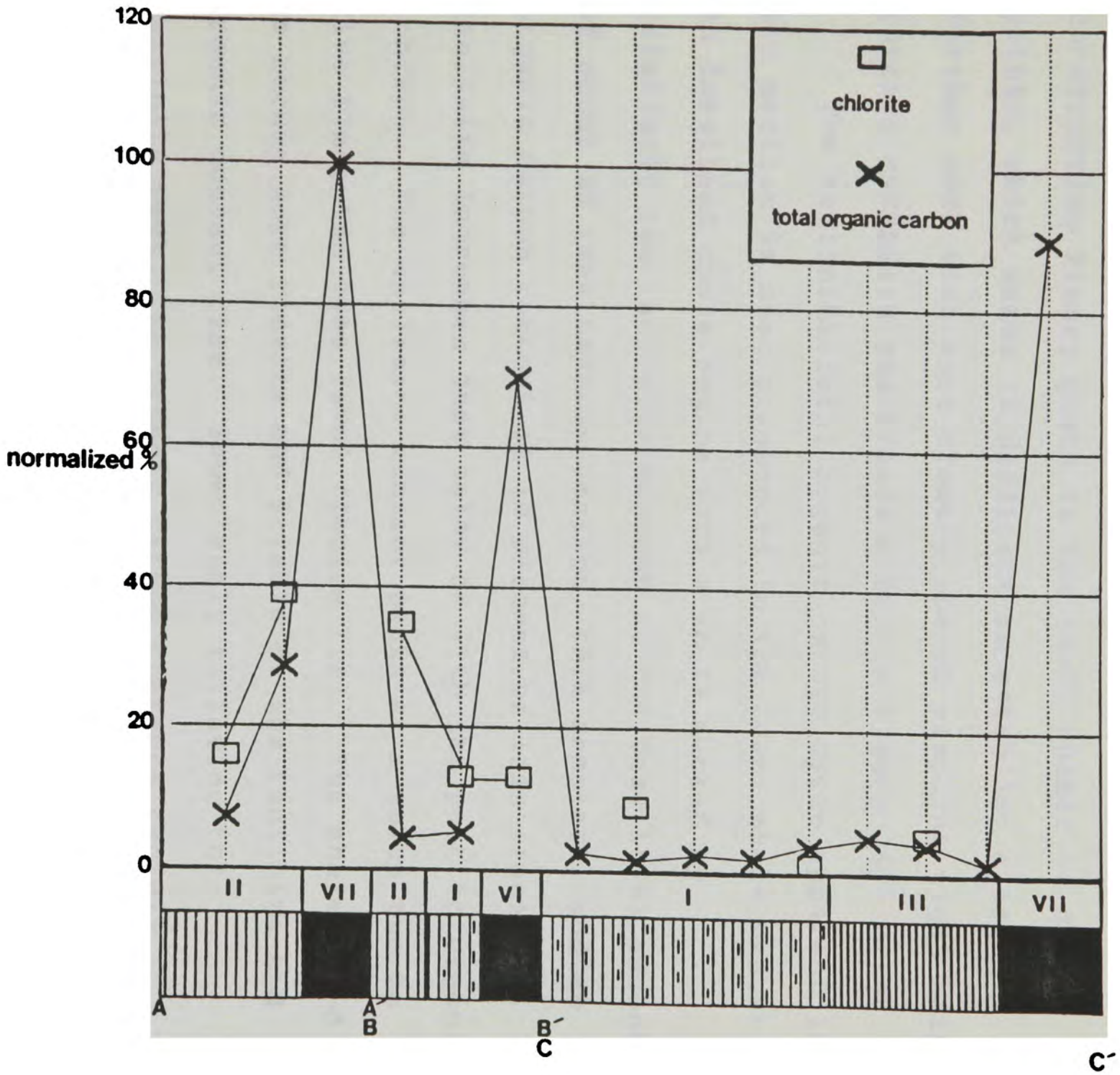
120
100
80
60
40
20
0
normalized %
chlorite
total organic carbon
II
VII
II
I
VI
I
III
VII
A
A'
B
B'
C
C'

kaolinite and total organic carbon is probably due to the large portion of the C-C' cycle with low total organic carbon content (Figure 13), which causes a cluster of data at the low end of the graph. Another problem with constructing binary plots is the small number of data points, which makes it difficult to establish a trend. Further work with more closely spaced sampling might help further establish the trends shown in Figure 26.

The kaolinite/total organic carbon cycle apparent in the section is most pronounced in the lower shale member. An idealized cycle begins with a shale marked by relatively low kaolinite content at the base level amount of about 25 (see methods section, this chapter), and an organic carbon content of 10 percent or less (facies I). Kaolinite increases just below or with the peak in organic content. The kaolinite content peaks at a value two to five times the base level (facies III). The shales tend to become more fissile and friable as the kaolinite and organic content rise. Immediately following this kaolinite peak, the organic carbon contents rapidly increases to form a lignite (facies VI-IX) with well developed fissility. Above the lignite bed, the cycle repeats itself.

Such cycles are of differing scale. The ideal cycle described above would span 9 meters or more of section (Figure 28). There are smaller cycles, such as A-A' and

Figure 28. Vertical section from A - C' in the lower shale member showing lithologic changes in the cycles.

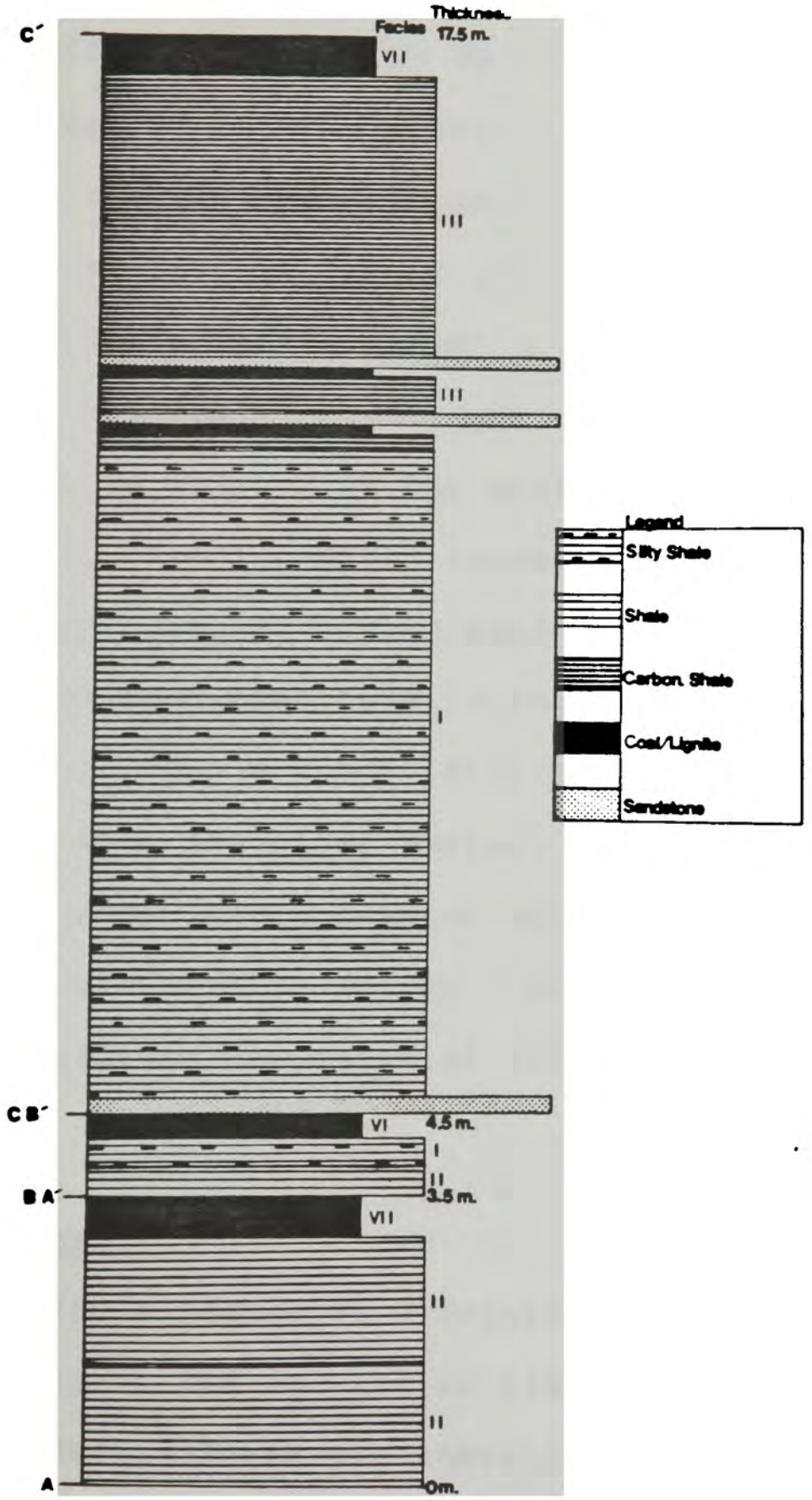
C´
Facies
Thickness
17.5 m.
VII
III
III
I
II
II
C B´
VI
4.5 m.
I
II
B A´
3.5 m.
VII
II
II
A
0m.
Legend
Silty Shale
Shale
Carbon. Shale
Coal/Lignite
Sandstone

B-B', that encompass only a meter or few meters of section (Figure 28). In the smaller cycles, facies II or V is immediately overlain by a clayey lignite (facies VII) or lignitic clay (facies VI), with no other shale facies present. The cycles do not always follow the ideal scenario. For example, the second short cycle in Figure 15 shows a facies IA shale immediately overlain by a lignitic clay (facies VI). Normally, facies IA shales are not intimately associated with lignites.

Three facies IA samples in the middle of the large cycle (Figure 4 - C-C') reacted strongly with HCl when treated for total organic carbon analysis. This indicates a higher carbonate content than in the other shales. These shales also have a higher silt and sand content, and fewer organics than the other facies. Silt and sand content is variable in the samples with a trend to increased silt and sand in facies I shales. Carbonate is a rare or nonexistent component of all but facies I shales.

Middle Shale Member

The middle shale member is 9 meters thick (Figure 4, Lithology chapter), and is similar lithologically to the lower shale member. There are three carbonaceous units

spaced evenly throughout the section giving it a rhythmic appearance similar to the lower shale. A strong drop in the smectite level two to three times less than any other sample is recorded in the first shale above the Rattlesnake Mountain sandstone. This could be due to some environmental factor such as reduced flood events or selective transport bias. It may also reflect a smectite with poorly developed crystallinity. However, neither the X-ray diffraction, nor petrographic analysis revealed if this was the case. Only in the middle shale member are pale red purple (5 RP 6/2) shales found. Analysis of one of these shales indicates a composition similar to the other shales, with the exception that chlorite is twice as abundant.

Upper Shale Member

The portion of the upper shale member studied on Rattlesnake Mountain is 50 meters thick (Figures 4, Lithology chapter, and 29). These shales are much poorer in organics than the other shale units. There are some lignite beds at the bottom of the upper shale and top of the Terlingua Creek sandstone, but, apart from these samples, only a few units display an organic content as high as 10 percent. The more organic-rich, brown-gray shales belong to facies V. The clay constituents throughout the upper shale member are very similar to the

Figure 29. Yellow weathering upper shale member (top unit). Terlingua Creek sandstone member underlies upper shale member, and overlies brown and green middle shale member.

rest of the section, with one exception. The kaolinite levels are stable around the base level of 20, and never reach the highest levels (approx. 135) seen in the lower shale. The majority of the upper shale represents facies IB shales.

Conclusions

The shales of the lower, middle, and upper shale members are dominated by smectite. Lesser amounts of kaolinite, chlorite, and illite occur in the samples along with various silt-sized detrital grains (see Petrography chapter). Total organic carbon content varies from less than 10 percent to nearly 100 percent. Kaolinite content is seen to parallel or closely precede increases in organic carbon levels. Chlorite appears to follow the same trend, but probably is influenced by the kaolinite abundance peak. Illite usually decreases when smectite exhibits a strong increase, but the relationship is not clear.

The lower and middle shale members both show cycles capped by facies VI-IX. Facies IA shale reacts with HCl, and has a relatively higher silt fraction than the other shales, perhaps indicating a higher energy marine environment. The upper shale member is more homogeneous than the lower units, is largely composed of facies IB shales, and is much poorer in organic carbon.

CHAPTER V

CARBON AND OXYGEN ISOTOPES

$\delta^{13}C$ of Organic Matter

Stable carbon isotopic ratios of organic matter in sediments reflect the source of the organic matter in a deposit. Analysis of the $\delta^{13}C$ ratios of the organic matter found in the Aguja shales and coals was made in an attempt to distinguish subenvironments within the section.

$\delta^{13}C$ and $\delta^{18}O$ of Shell Carbonate

Analysis of four oyster shells (Ostrea, Crassostrea, and Flemingostrea) was performed to help determine the paleosalinity of the shale facies.The shells analyzed in this study came from units just below and throughout the section (see Figure 3, Lithology chapter), and therefore give indirect evidence for the environment of the shale and peat deposition.

Methods

Organic Matter

The shale and coal samples selected for isotopic analysis range from very light gray shales to subbituminous coals (facies I-IX). The preparation and combustion procedures, as well as the analytical

equipment, are the same as those described in the Methods section of the Clays and Total Organic Carbon chapter.

Shell Carbonate

The invertebrate shells were ground to a fine powder, and heated to 500 ^{0}C to combust any organic carbon. Then 10 milligrams of sample were loaded into reaction tubes with phosphoric acid and reacted in reaction vessels attached under vacuum to the mass spectrometer (Parker, 1964).

General

A VG Isogas SIRA 12 mass spectrometer with a gas separating system was used to analyze the carbon isotope ratios. The $\delta^{13}C$ ratio was determined versus a lab standard which is calibrated against SMOW, SLAP, and GISP. $\delta^{18}O$ values were reported relative to SMOW and converted to PDB by the following equation (Faure, 1986)

$\delta^{18}O$ PDB = ($\delta^{18}O$/1.03086) - 30.86.

Precision, based on analysis of a standard with each run, is plus or minus 0.1 o/oo within each sample run.

$\delta^{18}O$ and $\delta^{13}C$ are measures of relative amounts of heavy and light isotopes of an element expressed in thousandths. The formula for δ is

δ = [(Rsample - Rstandard)/ (Rstandard)] * 1000

where "R" refers to the ratio of $^{13}C/^{12}C$ or $^{18}O/^{16}O$ (Craig, 1953).

A more negative δ value represents an increase in the amount of ^{16}O or ^{12}C relative to ^{18}O or ^{13}C (Faure, 1986).

Results

$\delta^{13}C$ of the Organic Matter

There is an 8 meter zone of relatively constant isotopic values, corresponding to the large cycle (Figure 4, C-C/) described in Chapter III, with isotopic signatures falling between -24 and -26 o/oo (Figures 30 and 31). These values probably represent a combination of sources of organic matter to the shale (as discussed later), and a relatively stable environment of deposition. The isotopic signature remains uniform through the lignite capping the section. The coals and lignites throughout the section do not share any particular isotopic value, but range from -23 to -27.8 o/oo.

The highest $\delta^{13}C$ value comes from the middle shale member just below the Terlingua Creek Sandstone. This corresponds to the pale red purple (5 RP 6/2) shales (discussed in the previous chapter) that are enriched in chlorite. These shales have a signature of -22.68 o/oo, perhaps indicating more saline conditions.

Data points in the upper shale seem to represent a terrestrial (isotopically lighter) environment. The

Figure 30. $\delta^{13}C$ ratios for organic matter from point A in the lower shale member to the sandstone capping the section in the upper shale member. Lithologic relationships depicted below the graph are not to scale.

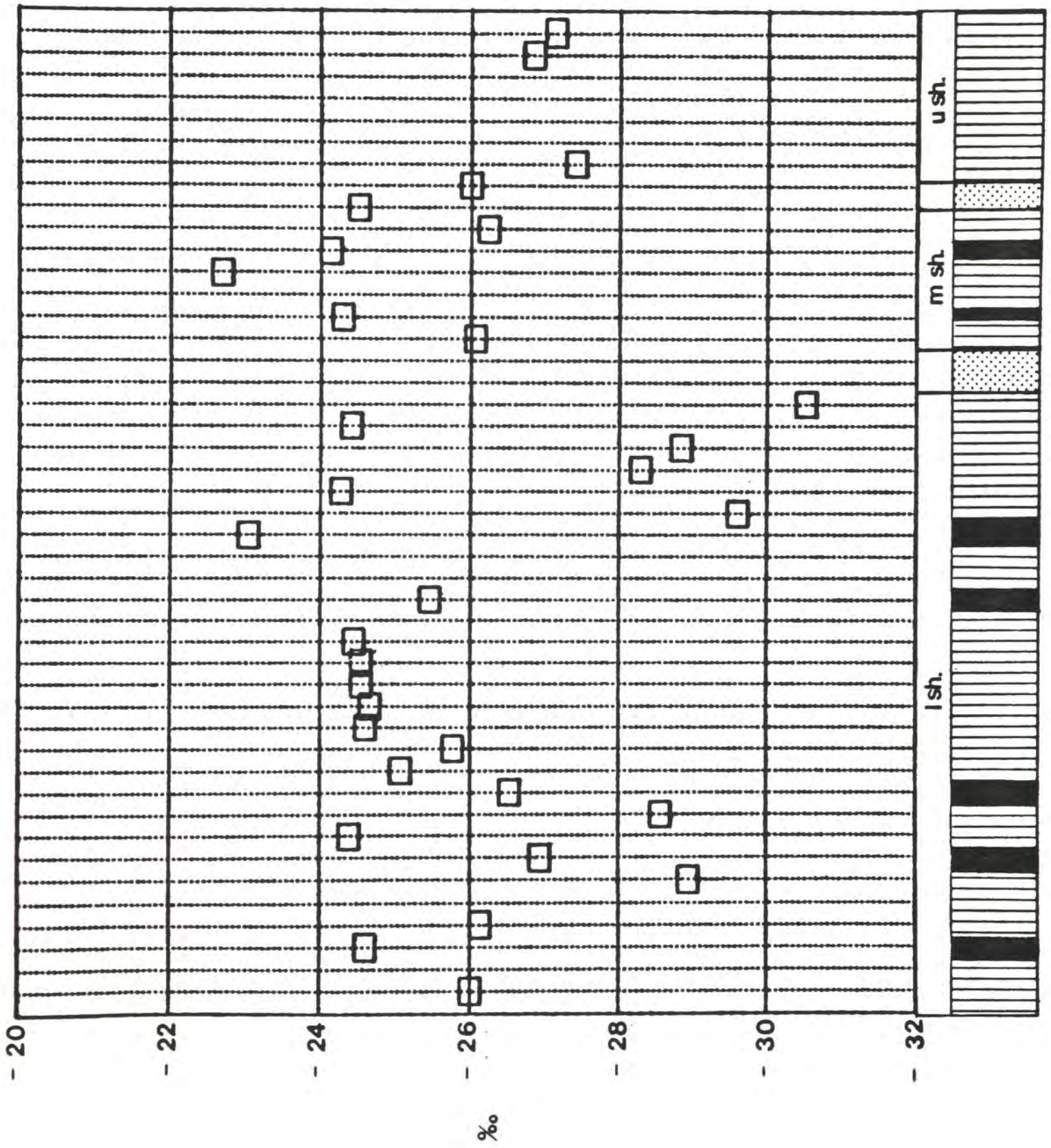
u sh.
m sh.
l sh.
- 20
- 22
- 24
- 26
- 28
- 30
- 32
‰

Figure 31. Relationship between $\delta^{13}C$ and total organic carbon from A - C' in the lower shale member. Facies relationships are not to scale.

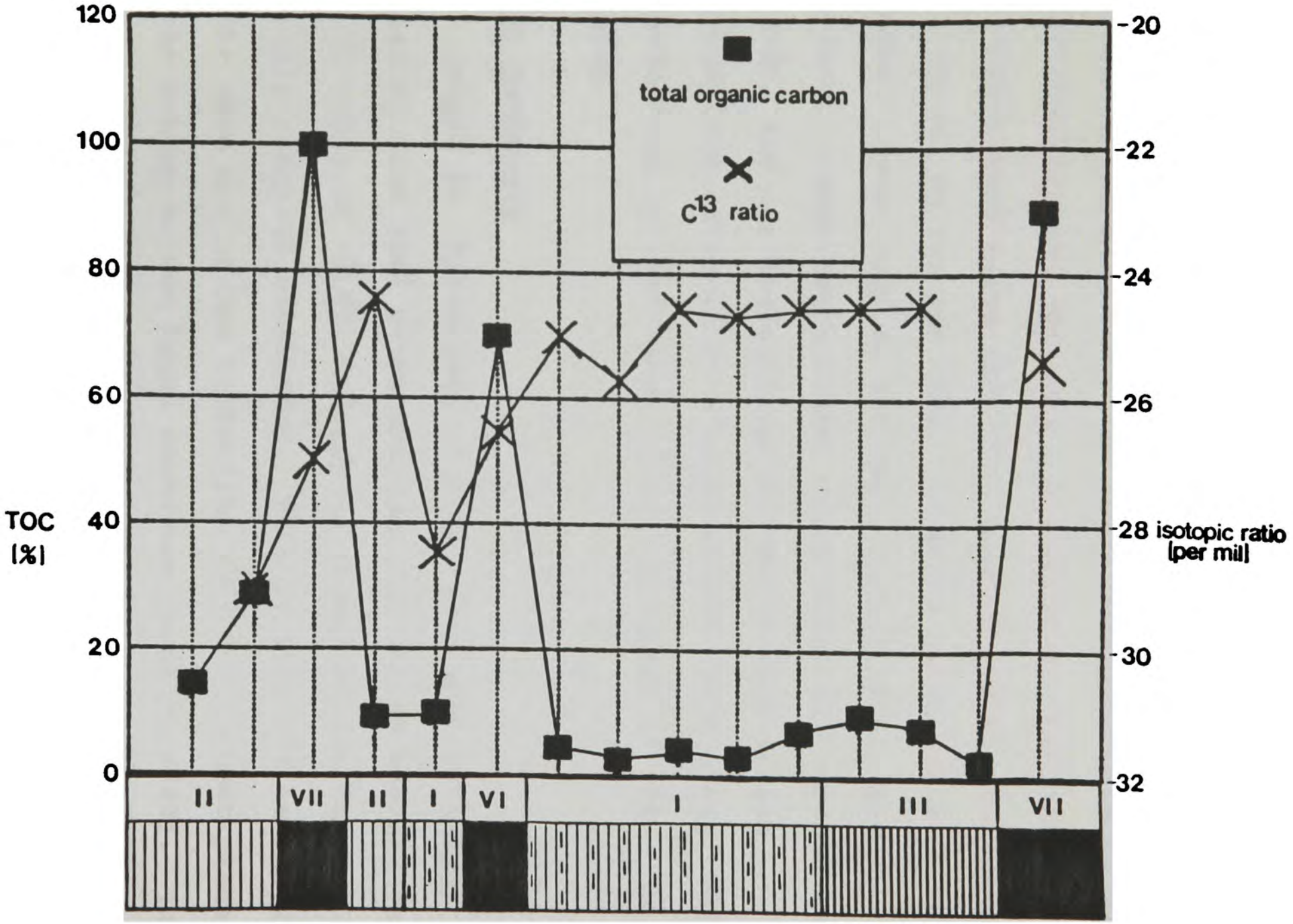
total organic carbon
C13 ratio
TOC [%]
120
100
80
60
40
20
0
-20
-22
-24
-26
-28 isotopic ratio [per mil]
-30
-32
II
VII
II
I
VI
I
III
VII

isotopic ratios are all more negative than -26 o/oo (except for one at the base of the section), indicating predominantly C_3 organic detritus.

Total organic carbon and the $\delta^{13}C$ values seem to be correlated (Figure 30) in the A-C' section described previously (see Clays and Total Organic Carbon chapter). $\delta^{13}C$ values follow the first two peaks relating to lignitic layers capping the small cycles (A-A'; B-B'). The total organic carbon then drops below 10% through most of C-C', and the isotopic ratio remains very stable through this interval at a value around -24.5 o/oo. The relationship is less clear through the rest of the section.

Shell Carbonate

Sample #1, Flemingostrea n.sp. (elongate variety), collected from just below the basal sandstone member, has a $\delta^{13}C$ value of -1.41, indicating normal marine to possibly brackish conditions. This corresponds to the top of the open marine Pen Formation, with the contact placed at the bottom of the basal sandstone (Lehman, 1985). The basal sandstone is a progradational sand unit, so a normal marine value below it is appropriate.

A thin shelled oyster, Ostrea sp. (sample #2), collected from a small channel sand in the lower shale has

a $\delta^{13}C$ signature of -4.87 o/oo. This would most likely represent a brackish to fresh water environment.

The Rattlesnake Mountain sandstone is a transgressive sandstone (Lehman, 1985). It rests unconformably on the lower shale, and is overlain comformably by the middle shale. A sample of Flemingostrea subspatulata (sample #3) from the Rattlesnake Mountain sandstone has a $\delta^{13}C$ signature of -0.19 o/oo, indicating normal marine conditions.

The last shell analyzed came from a shell lag near the base of the Terlingua Creek sandstone, which is a regressive progradational sand body (Lehman, 1985). The shell could represent material eroded from the middle shale. This shell of, Crassostrea subtrigonalis (sample #4), has a $\delta^{13}C$ ratio of -3.10 o/oo. This indicates that the oysters probably inhabited a brackish water environment. This is unexpected in view of the fact that the middle shale sits between the transgressive Rattlesnake Mountain sandstone and the regressive Terlingua Creek sandstone, and is laterally equivalent to marine shale (Lehman, 1985).

Discussion

Organic Matter

If the measured values have not been subsequently (diagenetically) altered, the isotopic ratios found in the

organic matter reflect a significant terrestrial organic carbon input into the marsh detritus. It is possible that mixing with either salt marsh detritus or marine detritus from algae or phytoplankton has occurred, resulting in an isotopic ratio that is in many cases intermediate between fresh and marine values. Mixing of organic matter in modern coastal marshes has been the subject of some research (Peterson et al., 1980; Fry and Sherr, 1984; Deluane, 1986), and no consensus has been reached. Marsh shales may receive organic detritus from terrestrial C_3 plants (-27 o/oo), fresh water particulate organic carbon (-28 o/oo), marine particulate organic carbon (-21 o/oo), chemautotrophic bacteria (-20 to -36 o/oo), and/or C_4 salt marsh grasses (-10 to -15 o/oo) (Fry and Sherr, 1984). Most models assume a mixture of marsh grass and terrestrial sources to determine relative contributions to the isotopic signature. A ratio of -24 o/oo would represent a possible mix of 75% terrestrial material, with a signature of -27 o/oo, and 25% salt marsh detritus, with a signature of -14 o/oo. Obviously, there are many ways to achieve the same ratio. The terrestrial or salt marsh grass signature could differ from typical values, or other sources mentioned could contribute to the isotopic ratio, with concomitant change in the percentages of contribution. It is likely, however, that mixing has occurred.

The details of organic matter mixing in the Late Cretaceous are unclear. C_4 grasses that inhabit modern marshes were not present during this time period, and it is not clear what plants did grow in the Late Cretaceous marsh. There is some evidence that monocots may have grown in the ancient marshes (see Palynology chapter), but this is not proven. The $\delta^{13}C$ signatures of the organic matter indicate that whatever plant did inhabit these ancient marshes, it may have had signature similar to modern marsh plants. It appears that the ancient marsh plants had more positive ^{13}C signatures than typical terrestrial plants.

Marine and terrestrial plants derive CO_2 from different sources with different isotopic ratios. Also, different types of plants follow different photosynthetic pathways to fix the carbon, resulting in distinctive signatures for different environments (DeLaune, 1986; Faure, 1986). Salt marsh species differ in isotopic signature from plants that live in fresh water or terrestrial environments due to the fact that salt marsh plants utilize a different pathway. Also, if marine organic material contributes detritus to a marsh, a distinct isotopic signature is produced.

In this study, there does not appear to be much order to the variations in the signatures (Figure 31), and little correlation with lithology, so distinguishing

facies or environments is very difficult. However, a few qualified observations are made. The $\delta^{13}C$ ratio expected for terrestrial organic matter ranges from -23 to -30 o/oo, with most species having a signature around -27 o/oo (Fry and Sherr, 1984). These plants use the C_3 (Calvin) Pathway (Calvin and Bassham, 1962) to fix atmospheric CO_2. The plants fix carbon from ribulose diphosphate into a three-carbon acid, utilizing the enzyme ribulose diphosphate carboxylase. These plants are called C_3 in reference to the three-carbon acid as the first product of photosynthesis. C_3 plants make up the bulk of terrestrial species.

The other main pathway utilized by plants during photosynthesis is called the C_4 (Hatch-Slack) Pathway. C_4 plants such as maize, sugarcane, marsh grasses, sea grasses, and tropical grasses follow this path which fixes a four-carbon acid as the first product of photosynthesis (Fry and Sherr, 1984; Hatch and Slack, 1966). CO_2 is first fixed into phosphoenolpyruvate to yield a four-carbon acid, using the enzyme phosphoenolpyruvate carboxylase. These plants display an isotopic signature that is heavier than the C_3 plants, ranging from -9 to -16 o/oo. Modern salt marsh grasses typically have a signature of about -14 o/oo.

Shell Carbonate

Carbon and oxygen isotopic ratios in shell material are thought to preserve an indication of the salinity of an environment. This is due to differing signatures of the source H_2CO_3 and HCO_3^- utilized by invertebrates in shell construction, as well as differing food sources (Clayton and Degens, 1959; Keith et al., 1964). The shells analyzed show variations indicating different salinity conditions (Figure 32) that can be related to conditions in the adjoining shales.

Molluscs fix carbon and oxygen in equilibrium with dissolved H_2CO_3 and HCO_3^- in the water, and thus reflect the environment in which they live (Fritz et al., 1986). Carbon isotopic values for marine invertebrates should range from +4.2 to -1.7 o/oo, and fresh water invertebrates should be lighter, with signatures ranging from -2.10 to -15.2 relative to the PDB standard (Keith et al., 1964). This is due to the initial differing donor signatures, with terrestrial sources being isotopically lighter than marine due to the sources of carbonate in the water. The δ O values for shell carbonate in marine invertebrates range from -3.0 to +2.98, and for freshwater invertebrates from -3.45 to -11.81 o/oo (Keith et al., 1964).

Figure 32. $\delta^{13}C$ and $\delta^{18}O$ signatures for various oyster shells from sandstones throughout the section (Figure 3). (l sh. = lower shale member; RMss = Rattlesnake Mountain sandstone member; m. sh. = middle shale member; TCss = Terlingua Creek sandstone member; u sh. = upper shale member).

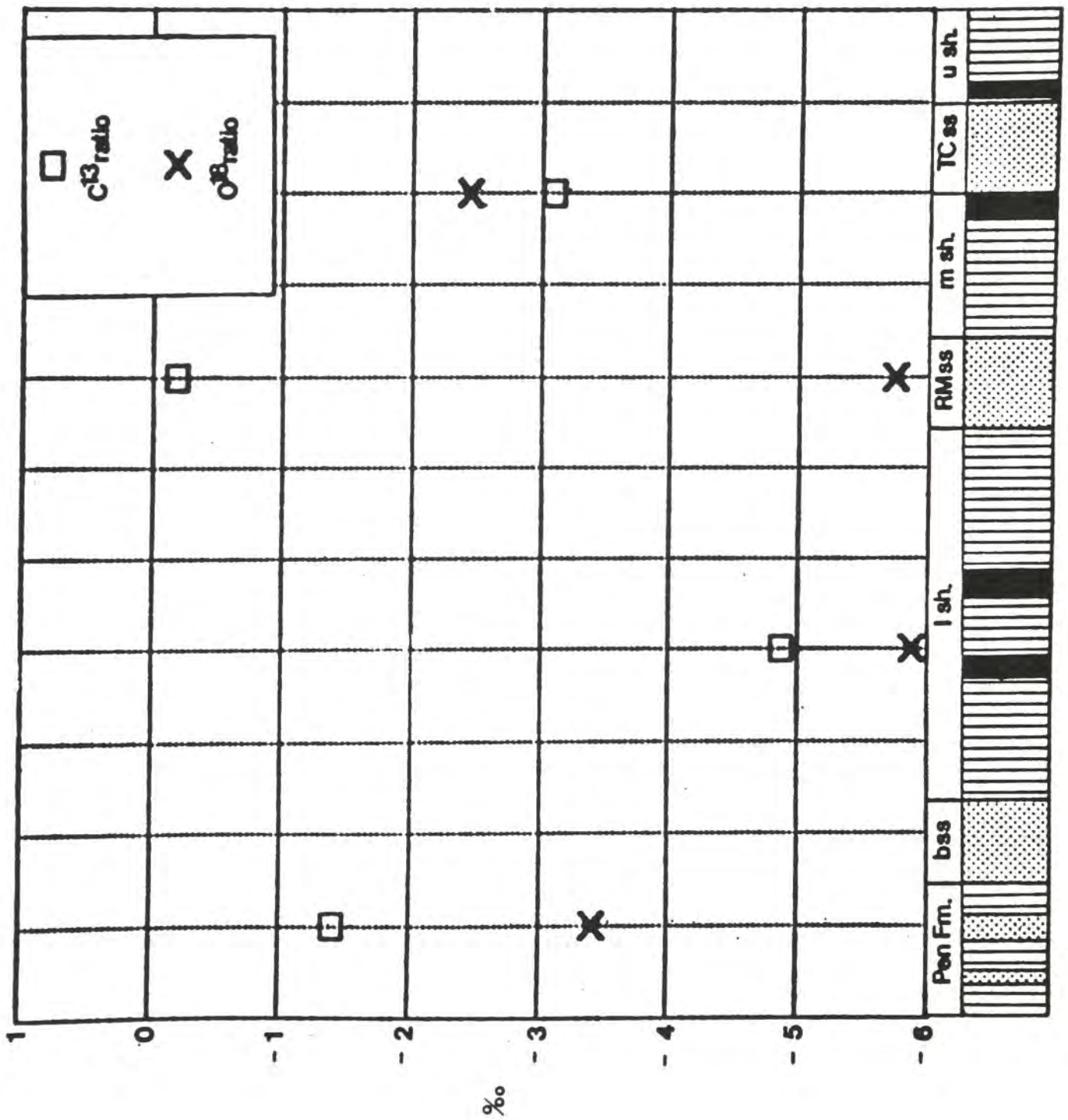
C^{13}_{ratio}
O^{18}_{ratio}
1
0
-1
-2
-3
-4
-5
-6
‰
Penn Fm.
bss
l sh.
RMss
m sh.
TCss
u sh.

The oxygen ratios do not support the salinities deduced from the carbon isotope data. The predictions only match for sample number 2. Shells 1,3, and 4 give indications that do not fit the environment expected from prior research or the environment predicted by the carbon ratios. There are several possible causes for this discrepancy. The $\delta^{18}O$ ratio of shell carbonate has been shown to be temperature sensitive (Urey, 1947). The Late Cretaceous was a relatively warm time period, so it is not reasonable to suggest the composition of sea water was influenced by fractionation caused by formation of ^{16}O-enriched polar ice caps. Wright (1987) calculated a $\delta^{18}O$ value of -1.22 o/oo for sea water due to dilution of the oceans by melting of the isotopically light polar ice caps. Oxygen isotope values can also be altered by post-depositional isotopic exchange with formation fluids. This is always a possibility, and there is some evidence that suggests the exchange processes may be less extensive for carbon isotopes (Clayton and Degens, 1959). The variability of the oxygen isotopes, combined with the fact that the carbon isotopes match environmental interpretations based on prior research (Lehman, 1985), and that the species in question are thought to be marine or brackish water invertebrates, indicates that the oxygen values may not accurately reflect the environment of deposition.

Problems

There are problems that must be addressed in using isotopic data for reconstruction of paleoenvironments. These problems include multiple organic sources, differing isotopic signatures of organic matter in the past, varying ratios of shell material isotopes reported by different workers, and alteration of isotopic ratios through diagenesis.

The problem of multiple organic sources has been discussed above. A simple mixing model, employed by most workers, may not take into account enough parameters to give an accurate picture of the contributions of the various sources donating organic detritus (Peterson et al., 1980; Fry and Sherr, 1984; Deluane, 1986). It is therefore necessary to recognize that, while mixing of the organic material may have occurred, the details of that mixing are not clear.

Another possible complication is that the isotopic ratios of marsh and swamp-forming organisms of the past may have differed from those of living species. This could be due to "age effects" (Hoefs, 1980) or an original difference due to vital effects in the plants.

There is some discussion that photosynthetic processes have experienced increases and decreases in intensity over time, creating "age effects" (Ronov, 1958; Hoefs, 1980). This results in isotope ratios that are

different in ancient plant material relative to today. This has not been widely accepted, and age effects should only influence the magnitude of individual values, preserving any trends.

Another factor affecting the uniformity of isotopic values over time is vital affects of the plants, causing different ratios than those seen today. This seems plausible except that environment, not species, is the dominant influence on isotopic ratios found in either plants or animals in the modern environment (Keith et al., 1964). Therefore, it would be reasonable to expect that modern salt marsh grass and terrestrial plants would share similar isotopic ratios with their ancient precursors. The apparent mixing of organic matter with a more positive $\delta^{13}C$ ratio with terrestrial organic material suggests that whatever plant inhabited the Late Cretaceous marsh, it may have had a signature similar to that of modern day marsh grasses.

A further complication involves varying isotopic signatures of carbon and oxygen in shell carbonate gathered by different workers. The isotopic signatures are usually similar to those mentioned above, but significant overlap is reported among marine and fresh water carbonate (Parker, 1964; Fry and Sherr, 1984; Wright, 1987). This obviously creates difficulty in

predicting environment based solely on isotopic signatures.

A more serious complication in isotope studies is that the isotopic signature of the organics may alter with time. Hoefs (1980) states that the $\delta^{13}C$ signature of organic matter is made more negative through time with the preferential destruction of ^{13}C-enriched carbohydrates and proteins. This leaves behind organic material that is relatively ^{12}C enriched, consisting of lipids, lignins, and cellulose. Organic matter older than Tertiary in age is thought to average around -28 o/oo regardless of its original signature. Hoefs (1980) provides no evidence for this statement; however, it is a serious consideration. If isotopic signatures become homogenized through time, they become useless as a descriptive tool. Craig (1953) reports isotopic values as old as Pennsylvanian in age ranging from -21.6 o/oo to -26.1 o/oo. Compston (1960) reports trends that are the inverse of those suggested by Hoefs, in Australian Permian coals in which the $\delta^{13}C$ increases with increasing age. The Permian coals range from -21 o/oo to -28 o/oo. Hoefs (Hoefs and Schidlowski, 1966) reports values for Precambrian organic material ranging from -22.34 o/oo to -32.80 o/oo. Obviously, not all organic matter suffers the same fate with time. The fact that the values for the upper Aguja shales range from -22.68 to -30.52 o/oo suggests that significant shifts of

the $\delta^{13}C$ signatures may not have occurred. Normal isotopic ranges for modern salt marshes range from -18 to - 27 o/oo (Peterson et al., 1980; Fry and Sherr, 1984; Deluane, 1986). If $\delta^{13}C$ shifts have occurred in the Aguja samples, they may have only slightly affected the magnitudes of the ratios, and not the trends.

Conclusions

The carbon isotopic signature of the organic matter in the shales and coals shows a wide range of values indicating various fresh to saline conditions. C_4 plants such as marsh grasses or reeds with more positive ratios, mixed with C_3 plants with more negative ratios, may have produced an isotopic signature with an intermediate value.

The isotopic signatures in the large cycle in the lower shale indicate a relatively stable environment with possible mixing as described above. The upper shale signatures indicate a fresh water environment with values lighter than -26 o/oo. Random negative and positive fluctuations may be due to varying terrestrial and marine organic influx during floods or storms.

The zone in the lower shale member corresponding to A-C' (Figure 4) demonstrates a possible relation between total organic carbon and the $\delta^{13}C$ value of the organic matter. The $\delta^{13}C$ value follows or parallels the total organic carbon content.

The $\delta^{13}C$ of shell material gives reasonable indications of the paleosalinity. The values indicate that the strata below the basal sandstone and in the Rattlesnake Mountain Sandstone were deposited in open marine conditions. The shells (from a channel in the lower shale, and in the top of the middle shale) indicate deposition in brackish water.

The $\delta^{18}O$ ratios of the shell carbonate are problematic and do not indicate the same salinity values as the carbon isotope ratios. It is possible that this may be due to variables that do not affect the carbon isotopic signature.

There are several assumptions that must be made, the most important being that the isotopic ratios in the organic material have not been altered with time. Various authors present conflicting evidence as to the reliability of isotopic ratios in organic matter older than the Tertiary, but, based on the range of values found here, it is assumed that little or no alteration has occurred. It is further assumed that, if alteration has occurred, only the magnitude of the values were shifted to lighter (more negative) values, and the trends are still preserved.

CHAPTER VI

PALYNOLOGY

Pollens and spores found in a sediment sample should reflect both the plants that live in or near the environment of deposition, and the regional flora. Although differential dispersal and survivability of palynomorphs bias the record of the local flora, identification of palynomorphs may at least provide an idea of the flora growing in the environment of deposition. The purpose of this part of the present study is only to identify the common forms present, and gauge their relative abundances. Palynomorphs in the carbonaceous units of the lower shale member of the Aguja Formation are dominated by angiosperm pollen. A diverse dicotyledonous and monocotyledonous assemblage is present. Gymnosperm pollen and moss spores are also present in minor amounts.

Methods

Carbonaceous shale and lignite samples from the lower shale member were selected for palynologic analysis owing to their high organic content. Palynomorphs were extracted using the methods described by Doher (1980). Samples were ground to an even powder with a mortar and pestle, placed in polyethylene tubes, and treated with HCl

to remove carbonate. The samples were rinsed with distilled water, centrifuged, and decanted four times to remove the acid. The samples were then treated with HF in a beaker, with an agitator, to remove silicates from the carbonaceous material. The samples were rinsed, centrifuged, and decanted as before.

Cellulose in the organic matter was then removed by acetylation. The samples were treated with glacial acetic acid to remove the water, and placed in a heated water bath with a 9:1 mixture of acetic anhydride and sulfuric acid. The samples were rinsed, centrifuged, and decanted as before. The procedure was repeated four times to remove as much cellulose as possible.

A drop of the residue containing unoxidized organic material and palynomorphs was then placed on a slide and allowed to dry. A cover slip was placed over the sample and glued with epoxy at the edges.

The slides were examined using a petrographic microscope with a 100X oil-immersion lens. The pollen and spores were stained by the organic material, and further staining was not necessary.

Identification of the pollen and spores was accomplished with a system using a combination of botanical affinity and artificial affinity as described by

Anderson (1960). A survey of papers edited by Kosanke and Cross (1966) also aided identification.

Results

A variety of tricolpate and triporate pollen grains are present. These palynomorphs represent dicotyledonous angiosperms. Figures 33a and 33b are examples of dicot pollen occuring in the lower shale member.

Monocolpate and monosulcate pollen grains are abundant. These palynomorphs represent monocotyledonous angiosperms. Two monocot palynomorphs are represented by Figures 34a and 34b. The monocot pollen are more numerous than any other group.

Gymnosperm pollen is rare, but fragments of vesiculate bladders indicate that they were present. Trilete spores are also rare, and probably pertain to Sphagnum (peat moss).

Conclusions

The shales and lignites of lower shale member of the Aguja Formation yield a pollen and spore assemblage dominated by a variety of dicotyledonous and monocotyledonous angiosperms. Occasional gymnosperm pollen and sphagnum spores are also found. The abundance of monocot pollen indicates that monocots may have been a major plant in the marsh community. Sphagnum moss may also have been part of the marsh flora. The dicot pollen

Figure 33. Photomicrograph of dicotyledonous palynomorphs (100X). a) ?Tricolporites b)?Tilia.

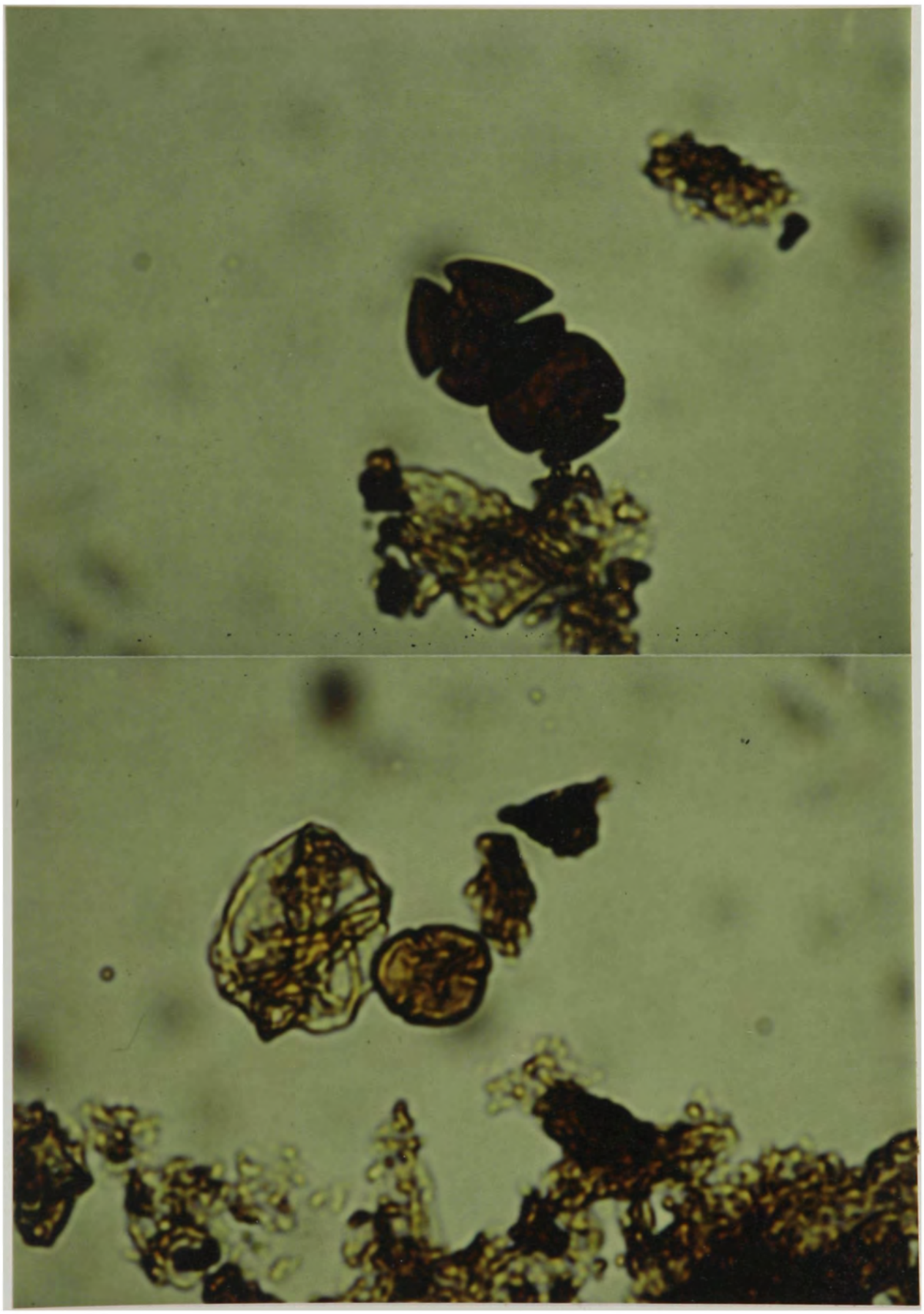

Figure 34. Photomicrograph of monocotyledonous palynomorphs (100X). a)?Arecipites b) ?Tetradites.

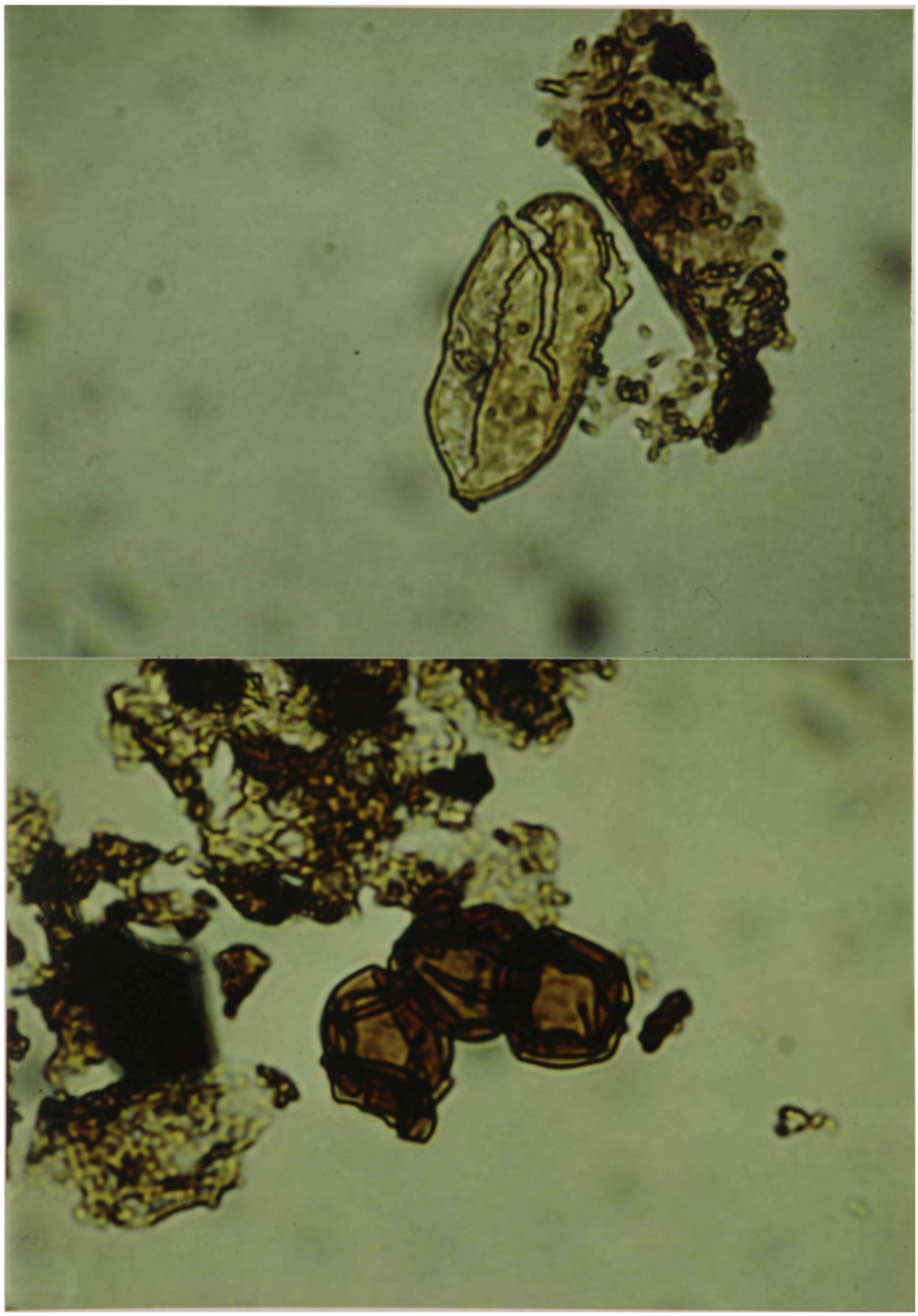

may represent arborescent or herbaceous flora growing inland or surrounding the marshes, or possibly as stands within the marsh itself. The rare gymnosperm pollen may represent part of the regional pollen "rain" derived from more remote upland regions.

This study indicates that identifiable palynomorphs can be extracted from these deposits. Further work is necessary, however, to establish the original floral community that inhabited these Late Cretaceous marshes.

CHAPTER VII

ENVIRONMENTS OF DEPOSITION

Fluvial sediment supplied to the Cretaceous Seaway during deposition of the Aguja Formation was dominated by clays derived from weathering of ash or felsic rocks from a volcanic source area in western Mexico. The large clay fraction of the sediment contributed to the formation of a muddy coastal setting with small prograding fluvial-dominated deltas (Lehman, 1985). The shales of the lower, middle, and upper shale members of the Aguja are dominated by smectite, but contain lesser amounts of kaolinite, illite, chlorite, silt-sized detrital material, and organic matter. The silt and sand sized detrital grain content varies widely, apparently with depositional setting. Facies defined on the basis of these components, as well as on stable isotope data, can be related to various subenvironments of a mud-dominated fluvial deltaic system.

Correlation of Facies and Environments

Interdistributary Bay

Facies I is divided into two subfacies representing different environments. Facies IA is marked by high silt content usually in laminations, and low organic carbon and

kaolinite content. It is variable in carbon isotopic signature and clay orientation. It normally contains macroscopic and microscopic concretions of hematite (Figure 35). Facies IA appears to represent deposition in interdistributary bays or standing bodies of water. Facies IB is similar to facies IA in color, organic content, and kaolinite content. It differs in that silt is evenly distributed within the samples. Hematite is only seen as poorly developed scattered microscopic concretions.

Deposition in a slightly higher energy tidal channel (Hine et al., 1988), interdistributary bay, or possibly a better drained marsh environment is suggested by high silt and low organic carbon content of facies IA. Samples from the lower shale member largely display clay orientation (birefringence fabric) that may have been caused by settling of the clay in relatively calm water. If the orientation is depositional, this would seem to negate a well-drained marsh environment, because root activity would have disrupted any orientation. Lamination is typical of facies IA shales, a further indication of deposition in calm water. Stable carbon isotopic signatures indicate a mixing of marine and terrestrial detritus in the organic matter. The facies IA isotopic values are slightly lower than average in the lower shale

Figure 35. Iron concretions in cycle C-C' in lower shale member facies IA shales.

member, perhaps indicating more saline or brackish water conditions. Common iron oxide and carbonate concretions also indicate saline to brackish conditions (Coleman, 1966). Such concretions represent syndepositional (pre-compaction) authigenic formation (Frey and Basan, 1978).

Deposition in a well-drained swamp environment may be represented by facies IB shales in the upper shale. Well-drained swamps produce shales with scattered lenses of silt, low organic content, and few concretions (Coleman, 1966). These features, in addition to in situ palm stumps (Figure 36a), prone logs (Figure 36b), poorly oriented clay, and terrestrial stable carbon isotopic signatures (-26 o/oo to -30 o/oo) indicate that these samples were likely deposited in a swamp environment.

Late Stage Bay Fill

Facies II and III represent deposition in a more reducing, organic-rich environment. These sediments may be a late stage bay fill or bay margin environment with plant growth in the bay. Plant growth reduces circulation, and contributes organic detritus. Such sediments may also represent a marsh that is poorly drained due to thickening plant growth, subsidence, or both. Facies II and III shales contain 10 to 20 percent organic carbon and isolated silt lenses. Carbon isotopic

Figure 36. Swamp deposits in the upper shale member of a) *in situ* palm stump (nickel as scale) and b) prone log (sunglasses as scale).

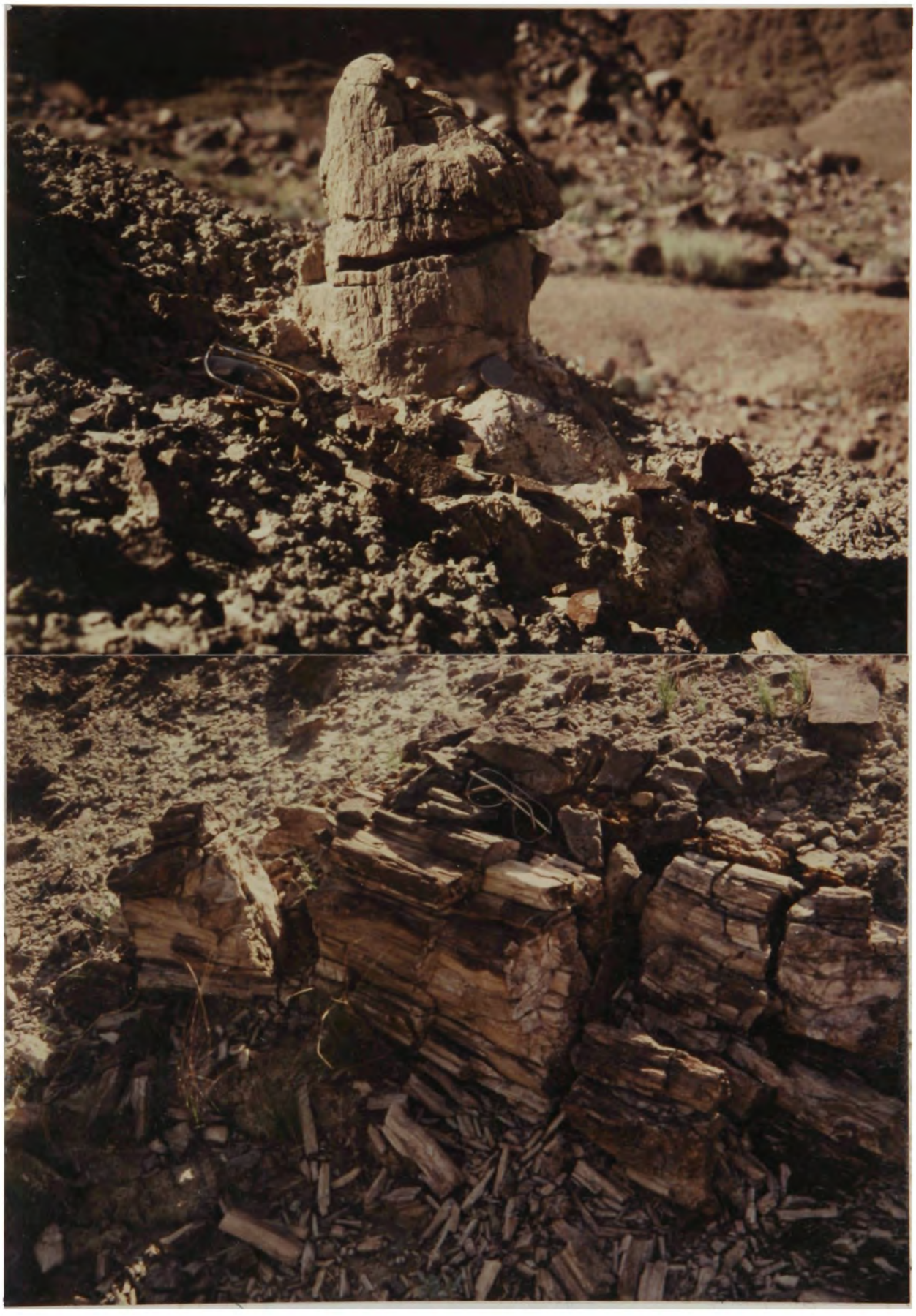

ratios are around -24.5 o/oo. These beds contain abundant carbonaceous flecks, and are dark gray (N 4) to light olive gray (5 Y 6/1) in color. These shales occur at the top of interdistributary bay deposits and in the middle of smaller depositional cycles. Clay orientation is normally poor, perhaps reflecting disruption of the clays by plant roots.

Immature Marsh

Facies IV and V represent an environment marked by dense plant growth and anoxic conditions. The shales have a total organic content ranging from 25 to 45 percent with abundant plant fragments and plant impressions (Figure photo). They are pale yellowish brown (10 YR 6/2) to brownish black (5 YR 2/1) in color, and contain scattered silt grains. Carbon isotopic ratios are variable, and reflect a mix of marine and terrestrial organic material. These units are often closely associated with climax marsh deposits.

Climax Marsh

Facies VI through IX represent a mature marsh environment marked by development of normally thin lignitic to subbituminous coal units. The lignites show well developed fissility and abundant fragments of carbonaceous material. Plant impressions in some of the lignites suggest reed or reed-like plants were present in

the marsh. Coalified wood fragments are found occasionally, especially in the lowermost coal. Absence or rarity of *in situ* stumps or prone logs in these deposits indicates that the woody material was probably brought in by fluvial processes. Carbon isotopic data on the coal and lignite is variable, perhaps indicating deposition in different marsh environments.

Sandstones Associated with Shales

A large distributary channel sandstone is present just above the basal sandstone member. Sandstone units within the shale are typically much smaller than this distributary channel unit. The sandstone units are lenticular and are cemented by calcite and kaolinite. These sandstones occasionally contain small oyster fossils that indicate a brackish water environment. These may represent small tidal channels dissecting the marsh as described by Hine et al. (1988). They may also represent minor deltaic distributary channels.

Summary

The facies of the lower, middle, and upper shale members of the Aguja Formation at Rattlesnake Mountain can be subdivided into environments of a prograding mud-dominated fluvial-deltaic system. The deposits represent a continuum of environments that range from probable interdistributary bay fill through various stages of marsh

growth to a well-drained swamp. Interdistributary bay fill and well-drained swamp deposits are similar in appearance, but differ in silt content, presence of laminations, and presence of iron concretions. Bay infilling and plant growth lead to development of immature marsh sediments that have increased higher organic carbon content. As infilling and plant growth continue, a climax marsh deposit forms that is characterized by a lignite or coal capping the cycle (Figure 37). The facies relationships described above are variable, with overlap of characteristics between facies. However, the facies are useful in defining changes in environment that result in facies characteristics.

Figure 37. Facies model illustrating ideal progradational sequence infilling bay.

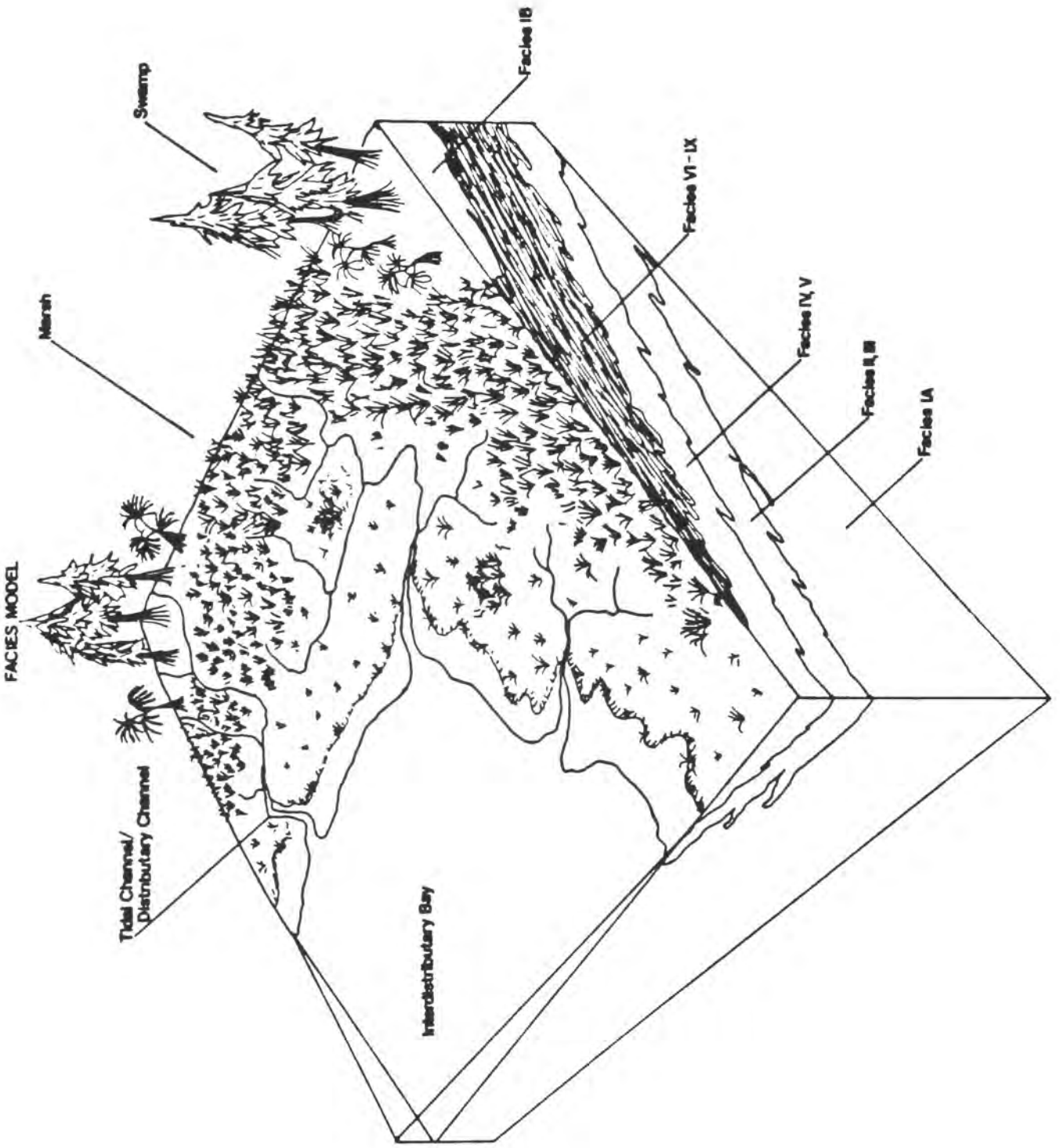
FACIES MODEL
Swamp
Marsh
Tidal Channel/
Distributary Channel
Facies IB
Facies VI - IX
Facies IV, V
Facies II, III
Facies IA
Interdistributary Bay

CHAPTER VIII

SUMMARY

The Aguja deltaic system appears unlike wave-dominated deltas typical of most of the Cretaceous Interior Seaway (Hubert et al., 1974; Weise, 1980). Barrier and strandplain sands typical of wave-dominated systems are not present in the Big Bend sequence, and varying thickness of the basal sandstone member indicates fluvial deltaic progradation (Lehman, 1985). The Big Bend deposits are similar to the fluvial-dominated deltaic deposits of the Late Cretaceous (Turonian) Ferron Sandstone member of the Mancos Shale in central Utah (Ryer, 1981), although the Aguja is less sand rich than the Ferron.

Reports of mud-dominated prograding coastlines are not common in the rock record or in present day settings. Ancient mud-dominated coastlines have been interpreted for the Late Cretaceous Highlight Muddy Field in the Powder River Basin (Berg, 1976), and the Irish Valley Member of the Upper Devonian Catskill Formation (Walker and Harms, 1971). Modern mud-dominated systems may be found off the coast of Suriname in South America, which receives fine-grained clastics from the Amazon River (Rine and Ginsburg, 1985), the coast of Kerala, India (Nair, 1976), and the

chenier plain of Louisiana (Coleman and Gagliano, 1964). These coastal plain environments differ in some respects, but all are prograding mud-dominated coastlines. A similar, but apparently non-prograding, mud-dominated system is found on the west coast of Florida as described by Hine et al. (1988). A similar environment might be represented by the chenier plain of Louisiana and the Atchafalaya River Delta (Coleman, 1966). Aguja lignites are not as continuous as are modern coastal plain peats, which can cover over 200 square miles (e.g., the Louisiana chenier plain; Coleman and Gagliano, 1964). This fact, combined with the presence of probable distributary channel sands indicates a deltaic environment for the lower and middle shale members of the Aguja.

Ancient and modern deltaic analogs may be found in many of the Tertiary and Pleistocene deltaic deposits of the Gulf Coast (Coleman, 1981). Fluvio-deltaic sedimentation in the Carboniferous of the eastern U.S. (Ferm, 1972) may represent a similar, though more sandy, environment. The Mississippi River Delta with its interdistributary bays, swamps, and marshes may be a modern analog, although on a much larger scale (Coleman, 1981).

Aquja Members

Lower Shale Member

The lower shale member contains many of the facies described above (see Environments of Deposition, chapter VII) as well as isolated distributary channel deposits. Lower shale deposition appears to be cyclic as reflected by the relationship between total organic carbon and kaolinite content. Kaolinite is enriched in layers directly underlying climax marsh facies, probably formed by leaching in the acid marsh environment. Acid leaching of alkalies and silica from existing detrital smectite and illite causes the formation of authigenic kaolinite in units underlying organic-rich layers (Moorehouse, 1959; Patterson and Hosterman, 1962; Staub and Cohen, 1978). Some workers suggest that such "underclays" were formed prior to deposition of coal-forming material as a result of prior sedimentation from source areas with soil development (Grim, 1935; Grim and Allen, 1938; Shultz, 1958). However, this does not explain repeated kaolinite enrichment below organic rich layers. Cyclicity in the section may reflect changes in local environment owing to autocyclic delta switching, subsidence, or variations in sediment influx. For instance, cycle C-C' (see Clays and Total Organic Carbon chapter) may represent the fill of an interdistributary bay (Coleman, 1966) that received increased sediment influx relative to the surrounding

marsh environment. As such bays fill, water depth decreases and allows the eventual colonization of the sediment by salt-tolerant plants. Continued sedimentation and plant growth leads to marsh development as described by Frey and Basan (1978). Eventually, accumulation of organic detritus in the reducing environment leads to peat formation. Reduced sedimentation due to accumulation of the marsh sediments and subsequent subsidence of the deltaic sediments, if rapid enough, may drown the marsh and cause repetition of the cycle.

Middle Shale

The middle shale member is very similar in appearance to the lower shale with lignitic units present, and may also represent largely a marsh environment. The middle shale is laterally equivalent to marine clays of the McKinney Springs tongue of the Pen Formation (Lehman, 1985). The middle shale member is underlain by the transgressive Rattlesnake Mountain sandstone member and overlain by the regressive Terlingua Creek sandstone member (Lehman, 1985). The "turnaround" point for the transgression appears to be near Rattlesnake Mountain to the southwest (Lehman, 1985), so this may represent the initial deltaic progradation over the Rattlesnake Mountain sandstone. Two marine foraminifera (Globorotaloides cf. conicus; Haplophraqmoides) occur in one unit of the middle

shale member indicates that marine shale intertongues with the marsh shales (Lehman, personal communication). A pronounced drop in smectite content occurs above the Rattlesnake Mountain sandstone member, and perhaps reflects segregation of the clays in the marine environment. A reduction in the amount of detrital clay due to reduced stream flow, or deposition in the distal portion of the marsh may be responsible for the smectite drop. Poor crystallinity of the smectite, causing lesser reflection during X-ray analysis and thus an apparent reduction in smectite content, is another possibility. The exact cause of the smectite reduction is not clear. Pale red purple (5 RP 6/2) shales near the top of the middle shale member have carbon isotopic values around -22.68 o/oo possibly indicating a more saline marsh environment. These shales also exhibit a chlorite content approximately three times higher than any other sample.

Upper Shale

The upper shale member is only partially exposed on Rattlesnake Mountain, but appears to represent a different environment of deposition. It is much less carbonaceous than the other members, and lignitic layers are only found in the lowest portions of the unit. The upper shale member consists largely of facies IB shales. Prone logs, palm stumps, carbon isotopic signatures typical of

terrestrial detritus, and a paucity of concretions indicate a well-drained swamp environment (Coleman, 1966). These deposits may resemble fresh water swamps as described from inland portions of the deltaic plain of the Mississippi River by Frazier and Osanik (1969).

General

Euhedral zircon and alkali feldspar crystals scattered throughout the section may have been derived either by weathering of felsic rocks in the source area, or possibly by weathering of volcanic ash. Volcanic eruptions in the magmatic arc present along the west coast of Mexico during Late Cretaceous time may have provided the source for these sediments. Siderite concretions and lense shaped aggregates are found in the lower and middle shale members. These are usually associated with organic-rich shales or lignites, but are also found in one lower shale sandstone. Siderite formation occurs in reducing environments, either in a freshwater environment where sulfate concentrations are initially low, or during diagenesis of marine sediments below the depth of sulfate diffusion. Therefore the siderite formation was probably restricted to the reducing marsh environment, and may reflect syndepositional or early post-depositional diagenesis. Iron and calcite concretions are common, especially in the lower shale member, and may have formed

member, and may have formed syndepositionally or soon after burial under the prograding saline marsh as described by Coleman (1966). Pollen and spores occuring in lower shale lignites indicate an angiosperm-dominated community. Abundant monocot pollen indicates that monocots probably inhabited the marsh environment. The stable carbon isotopic ratios of the organic matter is variable, with both positive (more marine) and negative (more terrestrial) spikes. These may be the result of marine organic material being transported onto the marsh during storms or by tidal activity (Hine et al., 1988), or terrestrial influx during floods.

CHAPTER IX

CONCLUSIONS

The Aguja Formation at Rattlesnake Mountain represents deposition in a mud-dominated fluvial-deltaic system with distributary channels, interdistributary bays, and delta plain marshes. Isotopic data, clay mineral analysis, petrographic analysis, total organic carbon data, and palynologic data, as well as lateral/vertical facies relationships, indicate that the depositional area was a system of muddy interdistributary bays, marshes, and swamps related to a prograding fluvial-dominated deltaic system.

The lower shale member contains concretions, intermediate isotopic values, apparent distributary channel sandstones, laterally discontinuous lignites, and plant material that are all consistent with an interpretation of a prograding delta plain marsh environment. Cyclicity of the deposits can be seen in the correlation between kaolinite and total organic carbon.

The middle shale member appears very similar lithologically to the lower shale member. It probably represents a similar depositional environment, perhaps a progradation of delta plain marsh sediments over the Rattlesnake Mountain sandstone member.

The upper shale member appears to represent a departure in depositional environment from the other shale members. *In situ* palm stumps, prone logs, high silt and sand content, low organic content, low kaolinite content, and terrestrial isotopic signatures indicate deposition in a well-drained swamp environment.

REFERENCES

Adkins, W.S., 1933, Mesozoic System in Texas, in The Geology of Texas, V.1, Stratigraphy, E.H. Sellards, W.S. Adkins, and F.B. Plummer (eds.), University of Texas Bulletin, Number 3232, pp.240-518.

Anderson, Roger Y., 1960, Cretaceous-Tertiary Palynology, Eastern Side of the San Juan Basin, New Mexico, State Bureau of Mines and Mineral Resources, New Mexico Institute of Mining and Technology, Memoir 6. 58 p.

Berg, R.R., 1976, Hilight Muddy Field - Lower Cretaceous Transgressive Deposits in the Powder River Basin, Wyoming, Mountain Geologist, V.13, pp.33-45.

Bohanan, J.P., 1987, Sedimentology and Petrography of Deltaic Facies in the Aguja Formation, Brewster County, Texas, Texas Tech University, Unpubl. M.S. Thesis.

Brindley, G.W. and Brown, G., 1980, Crystal Structures of Clay Minerals and Their X-Ray Identification, Mineralogical Society Monograph No. 5, Ch. 7, pp.430-431.

Brindley, G.W. and Kurtossy, S.S., 1961, Quantitative Determination of Kaolinite by X-Ray Diffraction, The American Mineralogist, V. 46, nos. 11-12.

Calvin, M. and Bassham, J.A., 1962, The Photosynthesis of Carbon Compounds, Benjamin Press, New York.

Clayton, R.N. and Degens, E.T., 1959, Use of Carbon Isotope Analyses of Carbonates for Differentiation of Fresh Water and Marine Sediments, Bulletin of American Association of Petroleum Geologists, V. 43, p.890.

Coleman, J.M., 1966, Recent Coastal Sedimentation: Central Louisiana Coast, Louisiana State University Studies, Coastal Studies Series, No.17, 73 p.

Coleman, J.M., 1981, DELTAS Processes of Deposition and Models for Exploration, 2nd ed., Burgess Publishing Co., Minneapolis, Minnesota. 124 p.

Coleman, J.M. and Gagliano, S.M., 1964, Cyclic Sedimentation in the Mississippi River Deltaic Plain, Gulf Coast Association of Geological Societies Transactions, V.14, pp.67-80.

Compston, W., 1960, The Carbon Isotopic Composition of Certain Marine Invertebrates and Coals from the Australian Permian, Geochimica et Cosmochimica Acta, V. 18, pp. 1-22.

Craig, H., 1953, The Geochemistry of Stable Carbon Isotopes, Geochimica et Cosmoschimica Acta, V.3, pp. 53-92.

Deluane, R.D., 1986, The Use of $\delta^{13}C$ Signature of C-3 and C-4 Plants in Determining Past Depositional Environments in Rapidly Accreting Marshes of the Mississippi River Deltaic Plain, Louisiana, U.S.A., Chemical Geology, V. 59, pp. 315-320.

Doher, L.I., 1980, Palynomorph Preparation Techniques Currently Used in the Paleontology and Stratigraphy Laboratories, U.S. Geological Survey, Geological Survey Circular 830. 29 p.

Faure, G., 1986, Principles of Isotope Geology, 2nd ed., John Wiley and Sons, Inc., New York.

Ferm, J.C., 1974, Carboniferous Environmental Models in Eastern United States and Their Significance, Geological Society of America, Special Paper No.148, pp.79-96.

Frazier, D.E. and Osanik, A., 1969, Recent Peat Deposits - Louisiana Coastal Plain, Geological Society of America, Special Paper No. 114, pp.63-86.

Frey, R.W. and Basan, P.B., 1978, Coastal Salt Marshes, in Coastal Sedimentary Environments, Davis, R.A. ed., Springer Verlag Publishing, pp. 101-169.

Fritz, P. and Fontes, J., 1986, Handbook of Environmental Isotope Geochemistry, V.2, Elsevier Publishing, New York.

Fry, B. and Sherr, E.B., 1984, $\delta^{13}C$ Measurements as Indicators of Carbon Flow in Marine and Freshwater Ecosystems, Contributions in Marine Science, V. 27, pp. 13-47.

Grim, R.E., 1935, Petrology of the Pennsylvanian Shales and Noncalcareous Underclays Associated with Illinois Coals, American Ceramic Society Bulletin, V. 14, No. 3, pp.113-119; No. 4, pp.129-134; No. 5, pp.170-176.

Grim, R.E. and Allen, V.T., 1938, Petrology of Pennsylvanian Underclays of Illinois, Geological Society of America Bulletin, V. 49, pp.1485-1514.

Hatch, M.O., Slack, R.C., and Johnson, H.S., 1967, Further Studies on a New Pathway of Photosynthetic Carbon Dioxide Fixation in Sugarcane and its Occurrence in Other Plant Species, Biochemical Journal, V. 10, pp.417-422.

Hine, A.C., Belknap, D.F., Hutton, J.G., Osking, E.B., and Evans, M.W., 1988, Recent Geological History and Modern Sedimentary Processes Along an Incipient, Low-Energy, Epicontinental-Sea Coastline: Northwest Florida, Journal of Sedimentary Petrology, V.58, No.4, pp.567-579.

Hoefs, J., 1980, Stable Isotope Geochemistry, 2nd ed., Springer-Verlag, New York, 208 p.

Hoefs, J. and Schidlowski, M., 1966, Carbon Isotope Composition of Carbonaceous Matter from the Precambrian Witwatersrand System, Science, V. 11, pp. 1096-1097.

Hubert, J.F., Butera, J.G., and Rice, R.F., 1974, Sedimentology of Upper Cretaceous Cody Parkman Delta, Southwestern Powder River Basin, Wyoming, Geological Society of America Special Paper, No.148, pp. 79-96.

Johns, W.D., Grim, R.E., and Bradley, W.F., 1954, Quantitative Estimation of Clay Minerals by Diffraction Methods, Journal of Sedimentary Petrology, V. 24, no. 4.

Keith, M.L. and Anderson, J., 1964, Carbon and Oxygen Isotopic Composition of Mollusk Shells from Marine and Fresh Water Environments, Geochimica et Cosmochemica Acta, V. 28, p.1757.

Keith, M.L., Anderson, G.M., and Eichler, R., 1964, Carbon and Oxygen Isotopic Composition of Mollusk Shells from Marine and Fresh-Water Environments, Geochimica et Cosmochimica Acta, V. 28, pp. 1757-1786.

Knebush, W.E., 1981, Evidence for Deltaic Environment of Deposition for the Aguja Formation (Upper Cretaceous), Southwest Texas, American Association of Petroleum Geologists Bulletin (abstr.), V.65, p.764.

Kosanke, R.M. and Cross, A.T., eds., 1966, Symposium on Palynology of the Late Cretaceous and Early Tertiary, Geological Survey of America, Special Paper 170, 396 p.

Kovschak, A.A., 1973, Igneous and Structural Geology of the Grapevine Hills, Big Bend National Park, Brewster County, Texas, University of Texas at Arlington, Unpubl. M.S. Thesis, 107 p.

Lehman, T.M., 1982, A Ceratopsian Bone Bed from the Aguja Formation (Upper Cretaceous), Big Bend National Park, Texas, University of Texas at Austin, Unpubl. M.S. Thesis.

Lehman, T.M., 1985, Stratigraphy, Sedimentology, and Paleontology of Upper Cretaceous (Campanian - Maastrichtian) Sedimentary Rocks in Trans-Pecos Texas, University of Texas at Austin unpublished Ph.D. dissertation, 299 p.

Maxwell, R.A., Londsdale, J.T., Hazzard, R.T., and Wilson, J.A.,1967, Geology of Big Bend National Park, Brewster County, Texas, University of Texas Bureau of Economic Geology, Publication 6711, 320 p.

McDowell, F. and Clabaugh, S., 1979, Ignimbrites of the Sierra Madre Occidental and Their Relationship to the Tectonic History of Western Mexico, G.S.A. Special Paper 180, pp. 113-124.

Mitchell, J., 1985, The Dictionary of Rocks, Elsevier Publishing, New York, 128 p.

Moorhouse, W.W., 1959, The Study of Rocks in Thin Section, Croneis, C., ed., Harper and Brothers, New York. 514 p.

Nair, R.R., 1976, Unique Mud Banks, Kerala, Southwest India, American Association of Petroleum Geologists Bulletin, V.60, pp.616-621.

Parker, P.L., 1964, The Biogeochemistry of Stable Carbon Isotopes in a Marine Bay, Geochimica et Cosmochimica Acta, V. 28, pp.1155-1164.

Patterson, S.H. and Hosterman, J.W., 1962, Geology and Refractory Clay Deposits of the Haldeman and Wrigley Quadrangles, Kentucky, U.S. Geological Survey Bulletin 1122-F.

Peterson, B.J., Howarth, R.W., Lipshultz, F., and Ashendorf, D., 1980, Salt Marsh Detritus: an Alternative Interpretation of Stable Carbon Isotope Ratios and the Fate of Spartina Alterniflora, Oikos, V. 34, pp.173-177.

Rine, J.M. and Ginsburg, R.N., 1985, Depositional Facies of a Mud Shoreface in Suriname, South America - a Mud Analogue to Sandy, Shallow-Marine Deposits, Journal of Sedimentary Petrology, V.55, No.5, pp.633-652.

Ronov, A.B., 1958, Organic Carbon in Sedimentary Rocks (in Relation to the Presence of Petroleum), Geochemistry, V. 2, pp. 510-536.

Ryer, T.A., 1981, Deltaic Coals of Ferron Sandstone Member of Mancos Shale: Predictive Model for Cretaceous Coal Bearing Strata of Western Interior, American Association of Petroleum Geologists Bulletin, V.65, pp.2323-2340.

Schwertmann, U. and Taylor, R.M., 1977, Iron Oxides, in Minerals in the Soil Environment, Dixon, J.B. and Weed, S.B. eds., Soil Science Society of America, Madison, Wisconsin. 948 p.

Shultz, L.G., 1958, Petrology of Underclays, Geological Society of America Bulletin, V.69, pp.363-402.

Staub, J.R. and Cohen, A.D., 1978, Kaolinite-Enrichment Beneath Coals: A Modern Analog, Snuggedy Swamp, South Carolina, Journal of Sedimentary Petrology, V.48, no. 1, pp. 203-210.

Udden, J.A., 1907, A Sketch of the Geology of the Chisos Country, Brewster County, Texas, University of Texas Bulletin, 93, 101 p.

Urey, U.C., 1947, The Thermodynamic Properties of Isotopic Substances, Journal of the Chemical Society, V. 4, pp. 562-551.

Walker, J.G. and Harms, J.C., 1971, The "Catskill Delta": A Prograding Muddy Shoreline in Central Pennsylvania, Journal of Geology, V.79, pp. 381-399.

Weise, B.R., 1980, Wave Dominated Delta Systems of the Upper Cretaceous San Miguel Formation, Maverick Basin, South Texas, University of Texas Bureau of Economic Geology, Investigation No. 107.

Williams, H., Turner, F.J., and Gilbert, C.M., 1982, PETROGRAPHY An Introduction to the Study of Rocks in Thin Sections, 2nd ed., W.H. Freeman and Co., San Francisco. 626 p.

Wright, E.K., 1987, Stratification and Paleocirculation of the Late Cretaceous Western Interior Seaway of North America, Geological Society of America Bulletin, V. 99, pp. 480-490.

APPENDIX

TABLE 1

TOTAL ORGANIC CARBON AND KAOLINITE DATA

Sample	Kaolinite (norm.%)	TOC (wt.%)		
8		100		
11A	16	45		
11B	21	50		
11C		85		
11D		25		
11E	22	14	A	
11F	45	29		
12		100	A'	
13A	20	9	B	
13B	31	10		
13C	97	70	B'	
13D		5	C	
13E	49	3		
13F		4		Lower Shale
13I		3		
13J	35	7		
13L		10		
13M	78	10		
15		90	C'	
18A		90		
18B		40		
18C	100	65		
18D		14		
18E	18	10		
18F		3		Rattlesnake Mountain
22A	11	42		sandstone
22B		9		
22C		10		
22E	38	12		Middle Shale
22F		70		
23A		10		
23B		90		
23C		80		Terlingua Creek
24A	19	10		sandstone
29B		2		
29C		3		Upper Shale

TABLE 2

ORGANIC CARBON ISOTOPE VALUES

Sample	C		
			Basal Sandstone
8-A	-24.91		
8A-2	-25.06		
11A	-25.58		
11A-2	-26.33		
11C	-23.63		
11C-2	-25.66		
11D	-25.93		
11D-2	-26.35		
11E	-24.04	A	
11F	-28.93		
12	-27.31	A'	
12-2	-26.18		
13A	-24.39	B	
13B	-28.57		
13C	-26.12	B'	LOWER SHALE
13C-2	-26.96		
13D	-25.07	C	
13E	-25.77		
13F	-24.59		
13I	-24.66		
13J	-24.53		
13L	-24.53		
13M	-24.45		
15	-24.62	C'	
15-2	-26.28		
18A	-23.04		
18B	-29.61		
18C	-24.26		
18C-2	-24.22		
18D	-28.29		
18E	-28.84		
18F	-24.41		
18G	-30.52		
18BSS	-23.73		Rattlesnake Mountain
22A	-25.35		sandstone
22A-2	-26.03		
22B	-24.29		Middle Shale
22E	-22.68		
22F	-24.24		
22F-2	-24.12		Terlingua Creek Sandstone

TABLE 2
(continued)

23A	-26.23	
23B	-24.83	
23B-2	-24.32	
23C	-26.01	Upper Shale
24A	-27.41	
29B	-26.84	
29C	-27.14	

TABLE 3

SHELL CARBONATE CARBON AND OXYGEN ISOTOPE VALUES

Sample	O	C
BB (#1)	-3.41	-1.41
13D (#2)	-5.88	-4.87
RM (#3)	-5.74	-0.19
22C (#4)	-2.45	-3.10

Note -
BB - from below basal sandstone member
13D - from middle of the lower shale member
RM - from the Rattlesnake Mountain sandstone member
22C - from base of the Terlingua Creek sandstone member

PERMISSION TO COPY

In presenting this thesis in partial fulfillment of the requirements for a master's degree at Texas Tech University, I agree that the Library and my major department shall make it freely available for research purposes. Permission to copy this thesis for scholarly purposes may be granted by the Director of the Library or my major professor. It is understood that any copying or publication of this thesis for financial gain shall not be allowed without my further written permission and that any user may be liable for copyright infringement.

Disagree (Permission not granted)	Agree (Permission granted)
_____	Richard L. Record
Student's signature	Student's signature
_____	12/10/88
Date	Date